ORCA – Online Research @ Cardiff

This is an Open Access document downloaded from ORCA, Cardiff University's institutional repository:https://orca.cardiff.ac.uk/id/eprint/159965/

This is the author’s version of a work that was submitted to / accepted for publication.

Citation for final published version:

Feliciano, Dirsa, Arroyo, Orlando, Cabrera, Tamara, Contreras, Diana, Valcárcel Torres, Jairo Andrés and Gómez Zapata, Juan Camilo 2023. Seismic risk scenarios for the residential buildings in the Sabana Centro province in Colombia. Natural Hazards and Earth System Sciences 23 (5) , pp. 1863-1890. 10.5194/nhess-23-1863-2023 file

Publishers page: http://dx.doi.org/10.5194/nhess-23-1863-2023

Please note:
Changes made as a result of publishing processes such as copy-editing, formatting and page numbers may not be reflected in this version. For the definitive version of this publication, please refer to the published source. You are advised to consult the publisher’s version if you wish to cite this paper.

This version is being made available in accordance with publisher policies. See http://orca.cf.ac.uk/policies.html for usage policies. Copyright and moral rights for publications made available in ORCA are retained by the copyright holders.

Nat. Hazards Earth Syst. Sci., 23, 1863–1890, 2023
https://doi.org/10.5194/nhess-23-1863-2023
© Author(s) 2023. This work is distributed under
the Creative Commons Attribution 4.0 License.

Natural Hazards and Earth System Sciences
Open Access

Seismic risk scenarios for the residential buildings in the Sabana Centro province in Colombia

Dirsa Feliciano[1,2], **Orlando Arroyo**[1,2], **Tamara Cabrera**[3,4], **Diana Contreras**[5,6], **Jairo Andrés Valcárcel Torres**[7], and **Juan Camilo Gómez Zapata**[8,9]

[1]Faculty of Engineering, Universidad de La Sabana, Chía 250001, Colombia
[2]Research Center on Disasters and Climate Change (CIDEC), Chía 250001, Colombia
[3]Research Center for Integrated Natural Disaster Management (CIDIGEN), ANID/FONDAP/15110017, Santiago 4860, Chile
[4]Department of Structural and Geotechnical Engineering, Pontificia Universidad Católica de Chile, Santiago 4860, Chile
[5]School of Earth and Environmental Sciences, College of Physical Sciences and Engineering, Cardiff University, Park Place, Cardiff CF10 3AT, UK
[6]School of Engineering, Faculty of Science Agriculture and Engineering, Newcastle University, Newcastle upon Tyne NE1 7RU, UK
[7]Faculty of Engineering, Universidad de La Salle, Bogotá 11121, Colombia
[8]Seismic Hazard and Risk Dynamics, GFZ German Research Centre for Geosciences, 14473 Potsdam, Germany
[9]Institute for Geosciences, University of Potsdam, 14469 Potsdam, Germany

Correspondence: Dirsa Feliciano (dirsafeag@unisabana.edu.co)

Received: 2 March 2022 – Discussion started: 9 March 2022
Revised: 3 December 2022 – Accepted: 4 April 2023 – Published: 24 May 2023

Abstract. Colombia is in one of the most active seismic zones on Earth, where the Nazca, Caribbean, and South American plates converge. Approximately 83 % of the national population lives in intermediate to high seismic hazard zones, and a significant part of the country's building inventory dates from before the nation's first seismic design code (1984). At present, seismic risk scenarios are available for the major cities of the country, but there is still a need to undertake such studies in other regions. This paper presents a seismic risk scenario for the Sabana Centro province, an intermediate hazard zone located close to the country's capital. An exposure model was created combining information from the Global Earthquake Model (GEM) Foundation, surveys, and the national census. Fragility and vulnerability curves were assigned to the building types of the region. A hazard model was developed for the region and 18 earthquake scenarios with a return period of 475 years were simulated using the OpenQuake (OQ) hazard and risk assessment tool to estimate damage and economic losses. In addition, a social vulnerability index (SVI) based on demographic information was used to assess the direct economic loss in terms of replacement costs. The results show that 10 % of all buildings considered in the region would experience collapse, and 7 % would suffer severe damage. Losses account for 14 % of the total replacement cost of the buildings and represent 21 % of the annual gross domestic product (GDP) of the region.

1 Introduction

Colombia is in one of the most active seismic zones on Earth, where the Nazca and Caribbean tectonic plates converge against the South American plate (Paris et al., 2000). The seismicity of the country is associated with the activity of the South American subduction zone along the Colombian Pacific, the Bucaramanga seismic nest (BSN), and several other active faults (Arcila et al., 2020). According to the Colombian Geological Service (SGC, its abbreviation in Spanish), approximately 83 % of the national population lives in areas with intermediate to high seismic hazard levels (AIS, 2010; Arcila et al., 2020).

Published by Copernicus Publications on behalf of the European Geosciences Union.

In addition to the hazard levels mentioned above, more than 10 million Colombians live in houses vulnerable to seismic events (Build Change, 2021). This situation stems from non-engineered buildings and informal constructions that account for between 60 % to 90 % of the country's residential building stock (Bonet et al., 2016; Yepes-Estrada et al., 2017). Due to these conditions, earthquakes have resulted in considerable economic and human losses in recent history. Examples include the M_w 5.5 Popayán earthquake in 1983 (Contreras, 2018) and the M_w 6.2 Armenia earthquake in 1999. In the first case, the earthquake caused 287 deaths and 7248 injuries and affected 150 000 people (Cardona et al., 2004; Lomnitz and Hashizume, 1985). This earthquake represented an estimated loss of 0.98 % of the gross domestic product (GDP) for that year (Cardona et al., 2004; AIS, 2009). In the second case, this event caused 1185 casualties and 8523 injuries (Naciones Unidas – CEPAL, 1999), and 35 000 buildings collapsed or experienced severe damage (Chávez-García et al., 2021). The estimated losses from this earthquake amounted to 1.9 % of that year's national GDP (AIS, 2009; Cardona et al., 2004). In such cases, field observations showed that the resulting damage was concentrated in old and historical buildings and in those built from low-quality materials and using inadequate construction techniques (Villar-Vega and Silva, 2017; Cardona et al., 2004; Macdonald et al., 2000; PAHO, 1983).

To help formulate mitigation strategies for earthquakes, risk management agencies and researchers have developed earthquake risk scenarios for different countries at the local, national, and global levels (Chaulagain et al., 2014, 2015; Silva et al., 2014a; Erdik et al., 2003; Nievas et al., 2022). Recently, a seismic risk assessment and a set of earthquake scenarios were developed for the residential building stock of Colombia's three largest metropolitan centers: Bogotá, Medellín, and Cali (Acevedo et al., 2020). In addition, probabilistic seismic risk assessments have been conducted in cities such as Medellín (Salgado et al., 2014) and Manizales (Salgado et al., 2017; Carreño et al., 2017). Despite these efforts, there is still a need to assess the expected consequences of potential earthquake events in other parts of the country. Therefore, this study presents the methodology and results of a seismic risk scenario for the Sabana Centro region, a zone made up of 11 municipalities located in the department of Cundinamarca, north of Bogotá, the capital of the country. Historical earthquakes have occurred in and affected this region. In 1644, a M_w 5.5 earthquake mainly affected churches and houses in Bogotá, and in 1743 a M_w 6.2 earthquake caused severe damage to the churches of Cota and Chía, two of the region's municipalities (JICA, 2002; Salcedo and Gómez, 2013), which saw intensities of VII being experienced (Mercalli scale) (SGC, 2021a).

The development of seismic risk scenarios involves three main components: (1) a set of ground motion fields estimated for a given earthquake rupture (seismic hazard model), (2) an exposure model defining the types of buildings in the study zone and their spatial distribution, and (3) a set of fragility and vulnerability functions that describe the seismic vulnerability of the buildings. The seismic vulnerability of a structure is a quantity associated with the likelihood of it suffering damage in the event of ground motion of a given level (Calvi et al., 2006). To simulate this vulnerability, fragility curves are associated with the type of construction employed for the buildings in the study area. This association allows the estimation of the probability of a building suffering different damage levels due to earthquake-induced ground motion, i.e., light, moderate, extensive, and collapse.

For the first component (i.e., the hazard), a national probabilistic seismic hazard model developed by the SGC was used to select the events of interest to estimate potential damage and expected losses. In addition, a model developed by the SGC that describes the spatial distribution of Vs_{30} values was considered as a proxy to account for ground motion amplification due to soil conditions (Choi and Stewart, 2005). Information available from the national census was used to create the exposure model. The methodology used in Yepes-Estrada et al. (2017) was followed to assign the number of buildings per municipality. Regarding the structural vulnerability of the building stock, a database of fragility functions developed for the residential building stock in South America by Villar-Vega et al. (2017) and those developed for global seismic risk analysis (Martins and Silva, 2021) were taken as a basis. Seismic risk scenarios were simulated using these three components as input for the OpenQuake (OQ) hazard and risk assessment engine (Silva et al., 2014b), from which the number of damaged buildings and associated economic losses were calculated.

One aspect of risk assessment frequently neglected is social vulnerability (SV). Post-disaster assessments have demonstrated that the extent of losses from disasters depends not only on the magnitude and duration of extreme natural events but also on the resilience of the population to rebuild their lives, livelihoods, and property (Chen et al., 2013; Schmidtlein et al., 2011; Contreras, 2016). The most vulnerable segments of a population are usually the most severely affected by extreme natural phenomena (Contreras et al., 2020b). Experiences from past earthquakes, such as the 2010 Haiti earthquake which resulted in 200 000 deaths (Boot et al., 2010) and 1.5 million homeless (Contreras et al., 2020a), have shown that casualties and building damages are higher among people who live in poorly constructed non-engineered buildings (Boot et al., 2010). In some cases, less-favored families may be forced to sell their income-providing assets to fulfill their immediate basic needs, even though they are less able to replace them. Moreover, the impact of natural phenomena may span generations, as parents may need to withdraw children from schools to help generate family income, thus limiting their future opportunities. Consequently, earthquake preparedness plans should consider that the consequences of these events have a greater impact on more vulnerable members of a community. According to data from

Table 1. Area, distribution of population, and population density of the 11 municipalities that make up Sabana Centro (DANE, 2018).

Municipality	Area (km^2)	Inhabitants	Population density (inhabitants km^{-2})
Cajicá	51	82 244	1613
Chía	79	132 181	1673
Cogua	136	22 067	162
Cota	55	32 691	594
Gachancipá	44	17 026	387
Nemocón	94	13 171	140
Sopó	111.5	25 782	231
Tabio	74.5	21 665	291
Tenjo	108	21 935	203
Tocancipá	73.51	39 996	544
Zipaquirá	197	130 537	663

the World Bank (WB), Colombia has a Gini index of 0.517, making it a country with a substantial level of income inequality (World Bank, 2022). In fact, the same study showed that Colombia's economy has the second most uneven distribution of income within Latin America, with only Brazil being higher. In Colombia, inequality goes beyond income level, as it is also present in aspects related to quality of life, such as social security, access to basic services, education, and so forth (Joumard and Londoño Vélez, 2013). These differences are visible throughout the country, and the Sabana Centro province is an example of this. This study, therefore, also considers social vulnerability (Cutter et al., 2003), which is represented as an index to adjust the economic losses due to structural damage.

2 Description of the study area

Sabana Centro is a region of Cundinamarca, Colombia, to the north of Bogotá, the country's capital. Cundinamarca is one of the four most populated regions of the country, and Sabana Centro is one of the provinces that contributes the highest population (18 %) and department GDP (32 %). The province comprises 11 municipalities (Fig. 1), and according to the 2018 National Population and Housing Census (CNPV, its abbreviation in Spanish), the number of inhabitants of the region is 539 295 (DANE, 2018). Table 1 presents the area and the number of inhabitants of the 11 municipalities that make up this region.

In addition to natural population growth in Colombia, the country's capital and several municipalities have experienced a greater increase in population partly due to the constant migration from neighboring Venezuela since 2015. The region of Sabana Centro has not been a stranger to this process, where in recent years, it has seen a significant demographic change in most municipalities (Sabana Centro Cómo Vamos, 2019). In 2015, the population density was 460 inhabitants km^2, and in 2018, it had risen to 527 inhabitants km^{-2}. This increase in population density means that there was a growth rate of 14.6 %, which is higher than the national average of 5.9 %. Among the municipalities, Chía, Cajicá, and Zipaquirá had the highest population growth with 64 % of the region's total population. The number of inhabitants in the region represents 18 % of the department of Cundinamarca (67 % in urban areas and 33 % in rural areas).

3 Description of input parameters

3.1 Seismic hazard

The SGC, in collaboration with researchers from the Geological and Mining Institute of Spain and the Global Earthquake Model (GEM) Foundation, developed a national seismic hazard model (Arcila et al., 2020). Overall, this national seismic hazard model comprises a set of tectonic environments and seismogenic sources. In that study, the seismicity of the Colombian territory was classified into four tectonic environments. Superficial events (cortical) correspond to events in the national territory down to depths limited by the upper crust–mantle boundary. Interplate earthquakes of the Colombian Pacific subduction zone correspond to earthquakes that occur in the area of contact between the Nazca and South American plates along the country's Pacific coast. Earthquakes in the Benioff area correspond to earthquakes inside the plate, which is subducting towards the east from the Colombian Pacific towards the country's interior. Bucaramanga's seismic nest corresponds to an area where earthquakes with moment magnitudes between M_w 4.0 and 5.0 usually occur at depths between 140 and 200 km (Prieto et al., 2012).

3.1.1 Definition of the earthquake scenarios

The Sabana Centro province is located close to seismic hazard sources of different tectonic regional types, as shown in Fig. 2. According to the national seismic hazard model developed by the SGC and the GEM Foundation, the Sabana Centro province is close to active shallow seismic sources (such as the Usme fault), intraplate events from the Benioff zone, and deep events from Bucaramanga's seismic nest (Arcila et al., 2020).

In this study, earthquake events are defined in terms of the magnitude, location, and geometric characteristics of their ruptures. For the determination of the magnitude and location of the events to be considered in the estimation of damage, events from the unified earthquake catalogue developed by the SGC (SGC, 2021b) within a radius of 200 km were considered. Figure 3 shows the events of the complete catalog, considering those from the seismic nest, as well as those from a cortical environment. The figure shows events at distances less than 50 km from the center of Tenjo near the surface with

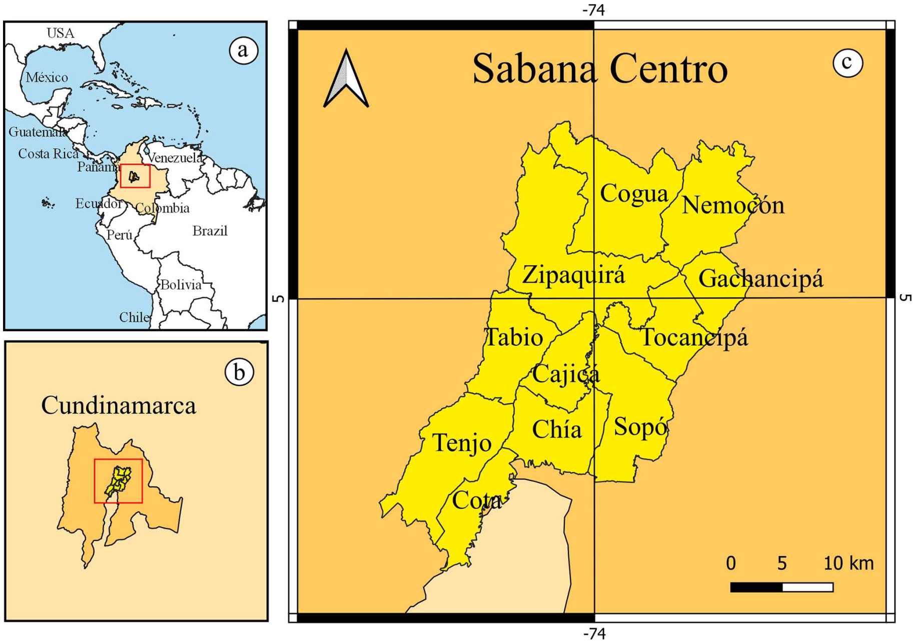

Figure 1. (a) Location of the study area within Colombia. **(b)** The region within the department of Cundinamarca (department is the first administrative division in Colombia). **(c)** The municipalities which make up the Sabana Centro province.

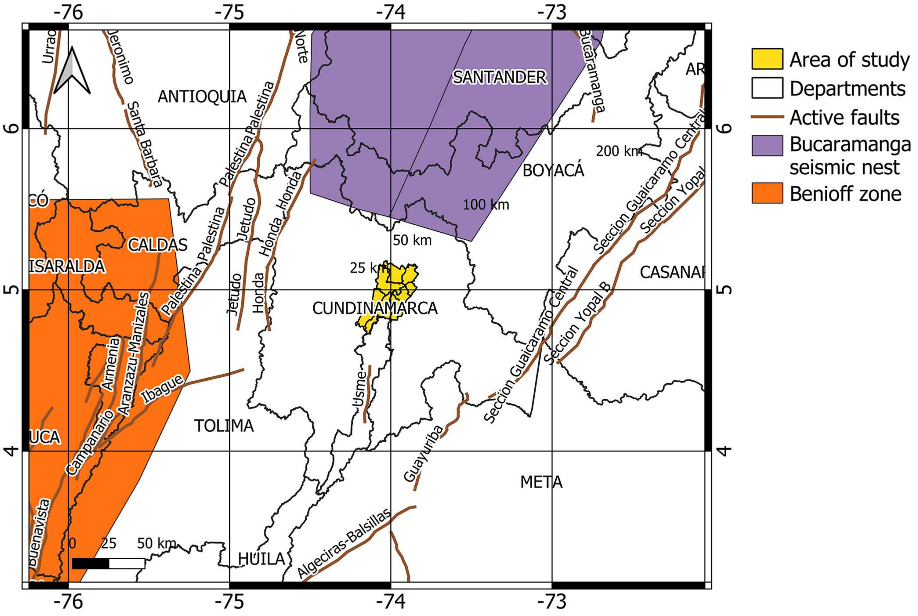

Figure 2. Seismic hazard sources close to the Sabana Centro province (Arcila et al., 2020): the active faults are presented in brown lines. The Usme fault is located less than 50 km from the municipality of Tenjo. The Benioff zone and the Bucaramanga seismic nest are located less than approximately 120 and 150 km from Tenjo.

depths less than 70 km and moment magnitudes ranging from M_w 4.0 to 5.5. There are also some events at depths between 70 and 300 km at distances between 50 and 100 km. These events range between a moment magnitude of M_w 4.0 and 6.5. It should be noted that most of the events in this area are shallow. Some far events at distances greater than 100 km are shallow events that can range between magnitudes of M_w 4.0 and M_w 7.0. It is also noted that there are deep events that can reach a moment magnitude of M_w 7.0.

To identify the type of event that contributes the most to the seismic hazard of the Sabana Centro province, a hazard disaggregation analysis (Bazzurro and Cornell, 1999) was

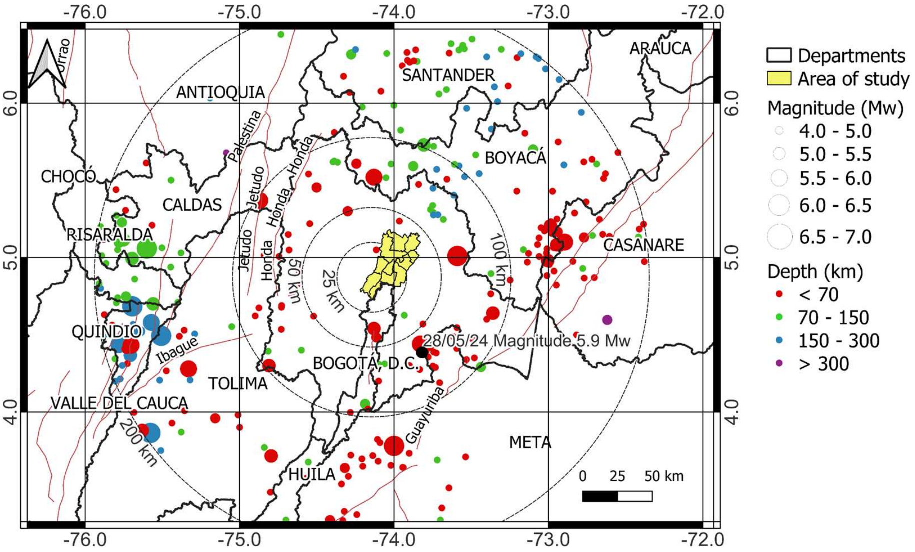

Figure 3. Geographic distribution of events occurring within 200 km of the study area selected from the unified earthquake catalogue of the SGC (SGC, 2021b). The size of the circle represents the magnitude of the event, and color indicates depth. The event marked with the black circle corresponds to the focal mechanism of the Quetame earthquake of magnitude M_{w} 5.9.

conducted using the OQ Engine, considering the national seismic hazard of Colombia (Arcila et al., 2020). Details of the seismic hazard disaggregation procedure are described in Pagani et al. (2014). The disaggregation was developed for a point within the region of analysis, which corresponds to the population centroid of the municipality of Tenjo (latitude: 4.872, longitude: −74.144), considering the Joyner–Boore distance to the projection of the rupture surface. The annual rate is 0.0021 (10 % probability of exceedance over 50 years or 475 years return period). Regarding the geometry of the earthquake ruptures, in the case of shallow events, the dip, strike, and rake angles were defined using available information from the seismic hazard model (Arcila et al., 2020), as well as the focal mechanism of the Quetame earthquake of magnitude M_{w} 5.9, which occurred in May 2008 (Páez et al., 2015).

The results obtained given the distance and magnitude of the earthquakes are presented in Fig. 4. In the case of the peak ground acceleration (PGA), crustal events make a higher contribution to the seismic hazard, located at distances less than 35 km, with magnitudes ranging between M_{w} 5.0 to 7.0. These events correspond to seismic sources of the crustal tectonic region type. A lower contribution is observed from events of the Benioff zone with magnitudes between M_{w} 6.5 and 7.0 at distances between 125 and 150 km. In the case of spectral acceleration with a period of 1.0 s (Sa (1.0 s)), the most significant contribution also comes from crustal events. However, there is an important contribution of events of magnitude greater than M_{w} 8.0 at distances ranging between 275 and 300 km, whose origins are in the subduction-interplate tectonic region.

Based on this disaggregation, 18 crustal events were selected from the probabilistic seismic hazard catalogue to be used in this study to calculate the expected damages and economic losses. The magnitude, location, and geometry of ruptures are shown in Table 2. The epicenter of each event is located within the municipality mentioned in the first column of Table 2 and shown in Fig. 5.

3.1.2 Soil–site conditions

To the best of the authors' knowledge, there are no specific studies of the seismic response of soil deposits within the region of Sabana Centro reported in the scientific literature. Therefore, the average shear wave velocity in the top 30 m (Vs_{30}) has been considered a proxy to address the contribution of soil–site conditions to the calculated ground motions at this regional scale (Derras et al., 2017). For designing the foundations of new buildings, the current Colombian seismic design code, NSR-10 (AIS, 2010), classifies soils based on the Vs_{30} values of the site of interest and proposes a set of coefficients to account for soil effects in the calculation of the seismic demand. Therefore, such ranges of Vs_{30} are considered for the Sabana Centro province. A map of Vs_{30} values within the Sabana Centro province is presented in Fig. 6, according to a map developed by Eraso and Montejo (2020), with a 7.5 arcsec resolution ($\sim 250\,\mathrm{m}^2$) based on digital elevation models. It shows the presence of different conditions, from soft soils with values of Vs_{30} under $200\,\mathrm{m\,s}^{-1}$ to stiff soils with $\mathrm{Vs}_{30} > 1000\,\mathrm{m\,s}^{-1}$. The figure also shows that most urban blocks are in sites with Vs_{30} values less than $450\,\mathrm{m\,s}^{-1}$. In particular, the municipalities of Tenjo, Tocan-

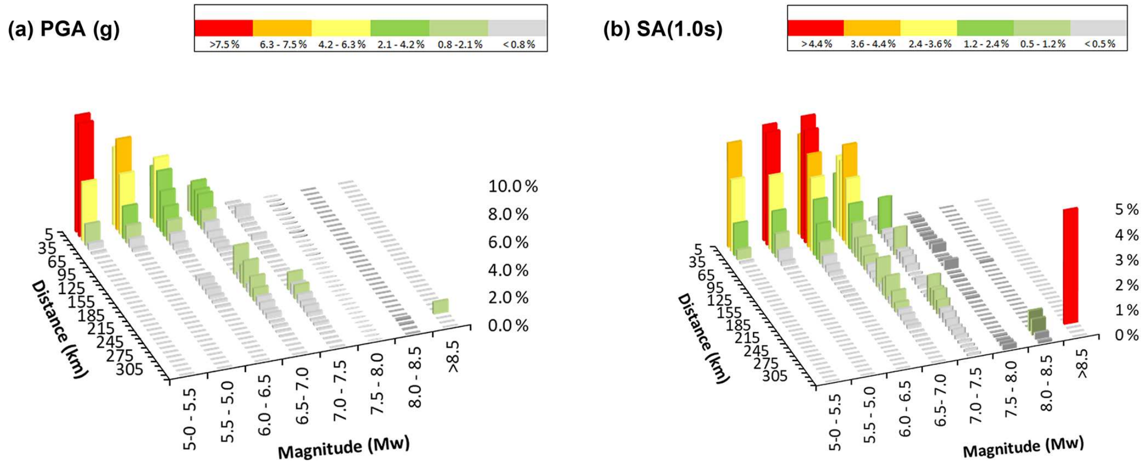

Figure 4. Contribution to the seismic hazard of earthquakes by distance and magnitude **(a)** PGA (g), **(b)** Sa (1.0 s). The color scale represents the percentage contribution of seismic events to the seismic hazard, with gray representing the lowest contribution and red the highest.

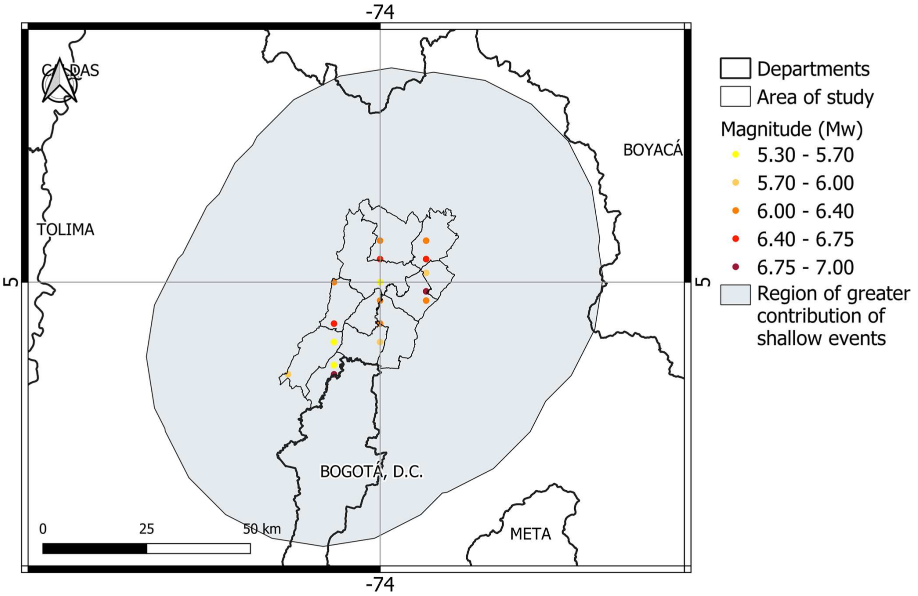

Figure 5. Location of the 18 selected events. The color range varies according to the magnitude of the timing of the events. The gray region represents the zone where shallow events have the largest contribution.

cipá, Nemocón, Gachancipá, Cajicá, and Chía are in areas with Vs_{30} less than 180 $m\,s^{-1}$, corresponding to soft soils.

3.1.3 Selection of ground motion prediction equations

Ground motion prediction equations (GMPEs) allow us to forecast the expected intensity of ground motion at a given site due to an earthquake event in terms of some measure, for example, spectral accelerations (Stewart et al., 2015). Several equations have been proposed worldwide for different tectonic environments, with different functional forms and input parameters. In Colombia, two sets of equations were developed to define the seismic hazard maps of the national building design code (NSR-10) (Gallego Silva, 2000) and the bridge design code (CCP-14) (Bernal Granados, 2014). More recently, Arcila et al. (2020) defined logic trees of GMPEs for the different tectonic regions of the country as a way to address epistemic uncertainty in the selection of other GMPEs, following the criteria proposed by Scherbaum et al. (2005) and Cotton et al. (2006), as shown in Table 3.

As introduced above, this study uses Vs_{30} to account for ground motion amplification due to soil conditions (Choi and Stewart, 2005). The values in this region range between 112 and 1100 $m\,s^{-1}$. This study considered crustal earthquakes, and among the three GMPEs proposed by Arcila et al. (2020) for shallow crustal regions in Colombia, the Idriss (2014)

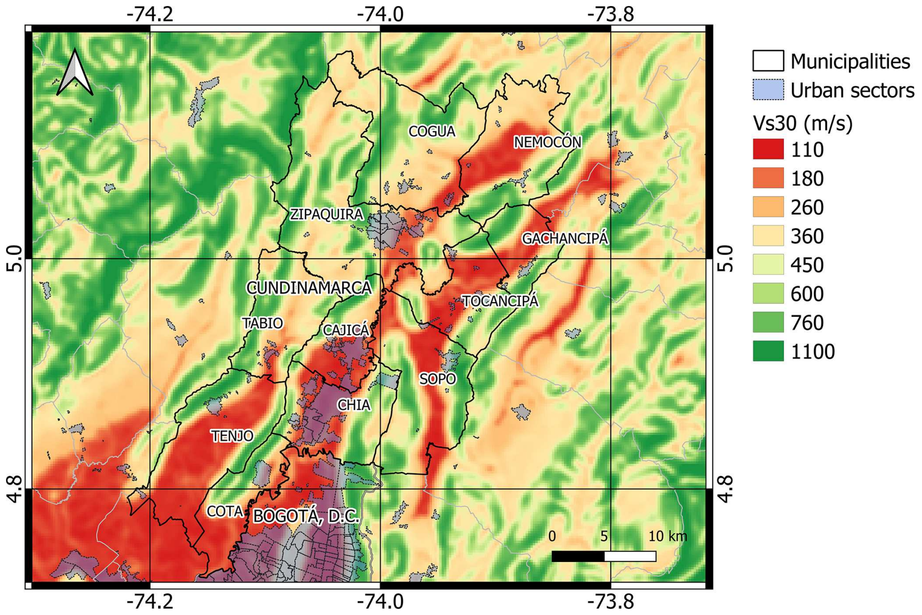

Figure 6. Spatial distribution of Vs_{30} values in the Sabana Centro province according to Eraso and Montejo (2020). The urban areas of the municipalities in the region are also shown.

GMPE is not defined for $Vs_{30} < 450\,\mathrm{m\,s^{-1}}$; therefore, it was not considered for the scenarios. The weight assigned to this model (0.399) was distributed proportionally between the Cauzzi et al. (2015, defined in the national model as Cauzzi et al. 2014) and Abrahamson et al. (2014) GMPE, whose final weights used in this study are 0.65 and 0.35, respectively.

Using the GMPE logic tree shown in Table 3, the mean expected PGA values for the Chía M_w 5.95 scenario of Table 2 may range between 0.12 g (Cogua) and 0.49 g (Cajicá).

3.2 Exposure model for the residential building stock

The building exposure model for the region has information about the building classes, the number of buildings, inhabitants, and the buildings' replacement costs. To develop this model for Sabana Centro, the methodology used by the South America Risk Assessment (SARA) project to develop exposure models in South America (Yepes-Estrada et al., 2017) was taken as a basis. The source of information to assign the number of buildings was the 2018 national census (DANE, 2018). The census allowed for having information on the number of dwellings and typical wall and roof materials, which were used to infer the different classes of buildings by municipality. A total of 156 628 dwellings were calculated; this number differs from that reported by the national census by 2.8 %, since it did not consider dwellings whose wall material is poured concrete. This material was not included, since there was no information available to relate it to any type of building class. The set of dwellings were related to the same building classes and same relationships ("mapping schemes") used in Yepes-Estrada et al. (2017). As the census information is reported in terms of dwellings, the procedure used in Yepes-Estrada et al. (2017) to calculate the number of buildings was also followed. Then, this data were complemented using information collected during remote surveys carried out by students from the Universidad de La Sabana in the municipality of Chía. The building replacement cost refers to the cost of structural and non-structural components of a building, and it is a value associated with the building's rehabilitation. This study has only considered the structural cost per building calculated based on cadastral information available in the Territorial Statistics System (TerriData, https://terridata.dnp.gov.co/index-app.html#/, last access: 28 December 2022) of the country. This replacement cost was computer per building, expressed in USD. As the currency in Colombia is in Colombian pesos, the exchange to US dollars was made for an average exchange rate of USD 4080. Figure 7 shows the results of inhabitants, buildings, and their total replacement cost for the region. The bold numbers indicate the percentages for each municipality.

A total of 75 778 residential buildings in the region were classified into 33 building classes. Table 4 provides a description of these typologies along with the number of buildings within each category and their percentages. Among them, 6249 randomly distributed buildings in Chía were inspected in 2020 by civil engineering students of the Universidad de La Sabana. Their attributes were collected, making use of the rapid remote visual screening (RRVS) web platform (Haas et al., 2016), which allowed the use of the GEM v.2.0 taxonomy (Brzev et al., 2013) as a checklist while observing the buildings' façades through Google Street View. The resulting dataset is available in Arroyo et al. (2022). Four attributes of

Table 2. Information describing the seismic events selected as scenarios in this work to estimate potential damage and impact.

Municipality	Magnitude (Mw)	Depth (km)	Strike (°)	Dip (°)	Rake (°)
Cajicá	6.35	5	0	90	0
Chía	5.95	5	0	90	0
Cogua	6.45	5.51	0	90	0
	6.35	5	0	90	0
Cota	6.95	9.27	39	76	−6.5
	5.55	5	0	90	0
Gachancipá	5.95	7.5	39	76	−6.5
Nemocón	6.65	6.78	0	90	0
	6.25	5	0	90	0
Sopó	6.55	6.11	0	90	0
	6.25	5	0	90	0
Tabio	6.65	6.78	0	90	0
	6.25	5	0	90	0
Tenjo	5.95	7.5	81	38	−76
	5.35	5	0	90	0
Tocancipá	6.85	25	81	38	−76
	6.15	5	0	90	0
Zipaquirá	5.65	5	0	90	0

Table 3. Logic tree of GMPEs for crustal events as defined by Arcila et al. (2020) for the national model and the actual weights used for the earthquake's scenarios.

Tectonic Region type	GMPE	Weight	
		Defined in the national model	Used for the scenarios
Shallow crustal	Idriss (2014)	0.399	0
	Cauzzi et al. (2014)	0.390	0.65
	Abrahamson et al. (2014)	0.211	0.35

the GEM v.2.0 taxonomy were used for classifying these inspected buildings: the main construction material type, material technology, lateral load-resisting system, the expected level of ductility, and the number of stories. During the elaboration of the surveys, instead of "labeling" buildings as certain typologies, the collected attributes were used to classify them in a probabilistic manner. For such a purpose, the method proposed in Pittore et al. (2018) was used to evaluate the level of compatibility between the observed building attributes and each predefined building typology. Details of this process can be consulted in Arroyo et al. (2022). This procedure allowed us to compare the percentages of the building classes calculated based on the SARA methodology and discretize the buildings by height.

From Table 4 it is noticeable that 58.60 % of the buildings are constructed of non-ductile unreinforced masonry walls, including adobe blocks and dressed and semi-dressed stone. In addition, 20.92 % of the buildings are from non-ductile confined masonry and 3.32 % are non-ductile reinforced concrete frames, for a total of 82.84 % non-ductile buildings. Figure 8 shows the number of buildings for the three types of construction materials identified in the exposure model: concrete, masonry, and wood. This figure shows that the predominant construction material is masonry (65 272 buildings), mainly in Chía and Zipaquirá, with more than 10 000 buildings for each one. Then, there are those buildings made of concrete (6745), with more than 1000 in Chía, Zipaquirá, and Cajicá. Last, there are those structures made of wood (3762), especially in Chía, with more than 990 units. The number of masonry buildings represents the 86.14 % of the total buildings in Sabana Centro, whereas those of concrete and wood represent 8.90 % and 4.96 %, respectively. The number of buildings for each of the 33 typologies is depicted in Fig. 9. In the case of concrete, the predominant building class is one story non-ductile reinforced concrete moment frames, while for the masonry buildings, the non-ductile unreinforced masonry wall class is predominant.

3.3 Physical vulnerability of residential building stock to seismic ground shaking

A large part of the building inventory was constructed using unreinforced masonry and with characteristics that make them non-ductile or with low ductility. Therefore, it is necessary to make an appropriate assignation of the fragility curves to evaluate their physical vulnerability to ground shaking. In the absence of specific curves locally developed for the Sabana Centro province, fragility curves available in the literature were selected to represent these structures. Thereafter, a literature review was undertaken to select the fragility functions that most closely resemble the characteristics of the Sabana Centro building inventory. The Physical Vulnerability Suite of the GEM Foundation (OpenQuake Platform – Vulnerability, 2021) was considered for the review. The GEM database for the specific case of Colombia has the curves developed by Acevedo et al. (2017) for unreinforced masonry houses constructed in Antioquia, Colombia. There are some curves for reinforced concrete buildings with geographical applicability in Manizales, Colombia, by Bonett Díaz (2003) and the dataset of Villar-Vega (2017) for South America. Although the set of curves covers different types of buildings, they are calculated based on different methodologies and different damage states.

Another available dataset of fragility curves is that developed by Martins and Silva (2021), who covered nearly 500 building classes at a global level including Colombia. The fragility is calculated from nonlinear dynamic analyses performed on equivalent single-degree-of-freedom (SDOF) oscillators. They considered four damage states that are also in-

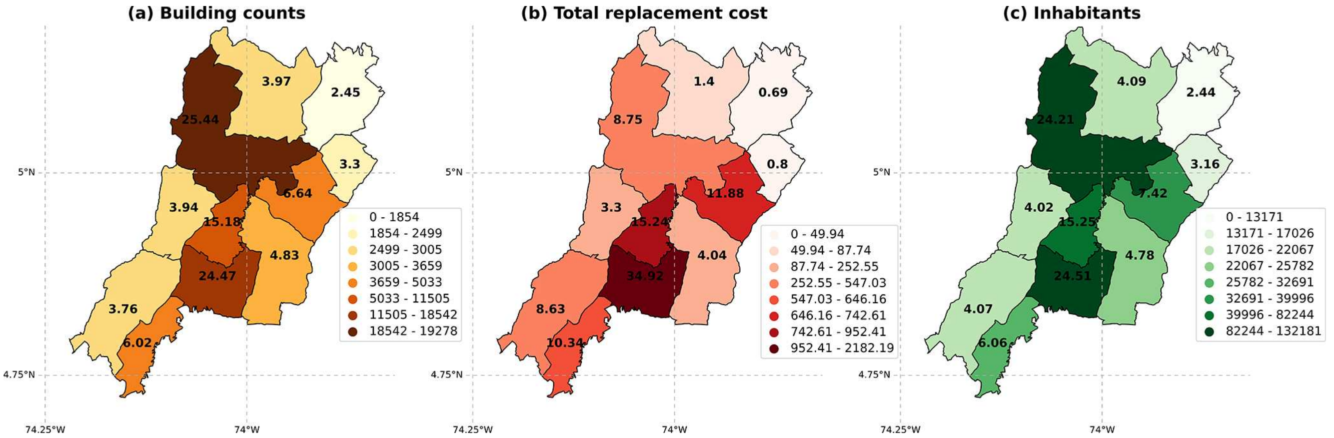

Figure 7. Summary of the exposure model for the Sabana Centro province. **(a)** Building counts, **(b)** total replacement cost in millions of USD, and **(c)** inhabitants per municipality.

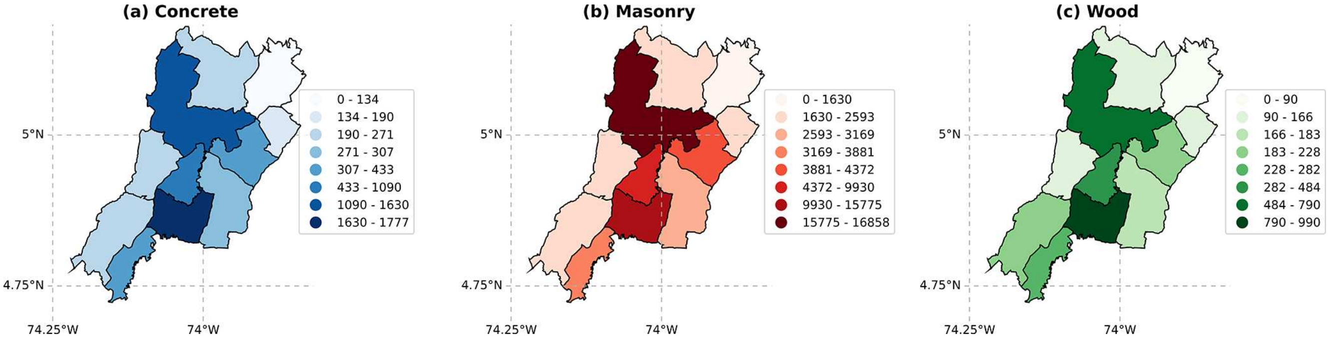

Figure 8. Spatial distribution of buildings whose construction materials are **(a)** concrete, **(b)** masonry, and **(c)** wood within each municipality.

tended to be studied in the present research: slight, moderate, extensive, and collapse. The corresponding damage thresholds were defined based on the spectral displacement of the structures. At a regional level is also the set of fragility curves for the residential building stock in South America (Villar-Vega et al., 2017), covering 54 common building classes. The methodology used for the derivation of the curves is similar to the one used in Martins and Silva (2021).

Based on the information collected, the fragility curves available in Martins and Silva (2021) were mainly used and complemented with those of Villar-Vega et al. (2017). These curves were selected in order to prevent a biased comparison of risk between the different municipalities in the region due to the different methodologies used to develop the fragility curves.

Therefore, a set of 33 fragility functions was used to represent the probability of exceeding a level of damage conditioned to ground-shaking intensity. These functions are comprised of 28 sets of curves reported by Martins and Silva (2021) and five sets developed by Villar-Vega et al. (2017). The last one is assigned to non-ductile confined masonry, one, two, and three stories, and ductile light wood members, one and two stories, since in the former these building classes were not included. These fragility functions are described by a cumulative probability curve with a log-normal distribution, and examples of some of them are presented in Fig. 10. This set of fragility curves was used to calculate the damage to the buildings included in the exposure model. Based on these curves, vulnerability functions were developed to evaluate the losses in the region. The loss ratios used in this study are 2 %, 10 %, 50 %, and 100 % for the slight, moderate, extensive, and collapse damage, respectively.

3.4 Social vulnerability (SV)

To determine the level of social vulnerability (SV) of the municipalities of the Sabana Centro province, this paper estimated a social vulnerability index (SVI) based on the methodology proposed by Cutter et al. (2003). The social equivalent to a quantitative physical risk assessment for earthquakes is an SVI. Social vulnerability is the reason for the different experiences of communities regarding the consequence of earthquakes (Burton and Silva, 2016). The construction of composite indicators based on the mathematical combination of a set of indicators, which consists of a

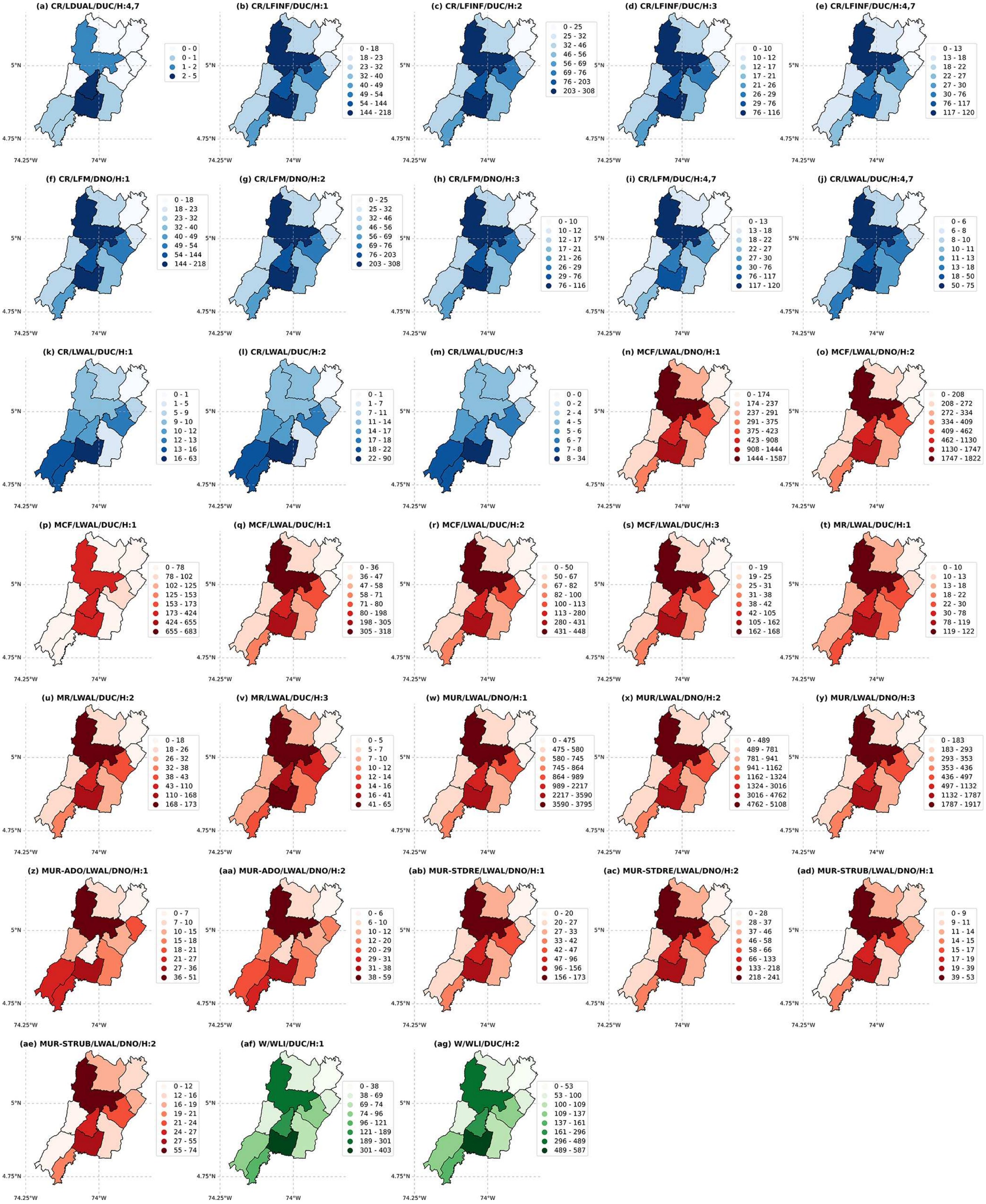

Figure 9. Spatial distribution of the building counts per class within each municipality.

Table 4. Summary of the building typologies in the exposure model defined for the study area. The building classes are defined based on the GEM v.2.0.

Building class	Description	Number of buildings	Proportion (%)	Replacement cost (USD in millions)
CR/LDUAL/DUC/H:4,7	Ductile reinforced concrete dual frame-wall system, four to seven stories	14	0.02	34.94
CR/LFINF/DUC/H:1	Non-ductile reinforced concrete infilled frames, one, two, and three stories	855	1.13	557.05
CR/LFINF/DUC/H:2		1207	1.59	786.42
CR/LFINF/DUC/H:3		453	0.60	294.91
CR/LFINF/DUC/H:4,7	Ductile reinforced concrete infilled frames, four to seven stories	464	0.61	1131.06
CR/LFM/DNO/H:1	Non-ductile reinforced concrete moment frames, one, two, and three stories	855	1.13	557.05
CR/LFM/DNO/H:2		1207	1.59	786.42
CR/LFM/DNO/H:3		453	0.60	294.91
CR/LFM/DUC/H:4,7	Ductile reinforced concrete moment frames, four to seven stories	464	0.61	1131.06
CR/LWAL/DUC/H:4,7	Ductile reinforced concrete walls, four to seven stories	292	0.39	715.24
CR/LWAL/DUC/H:1	Ductile reinforced concrete walls, one, two, and three stories	163	0.22	170.02
CR/LWAL/DUC/H:2		230	0.30	240.03
CR/LWAL/DUC/H:3		86	0.11	90.01
MCF/LWAL/DNO/H:1	Non-ductile confined masonry, one, two, and three stories	6154	8.12	1388.94
MCF/LWAL/DNO/H:2		7055	9.31	1713.00
MCF/LWAL/DNO/H:3		2646	3.49	642.37
MCF/LWAL/DUC/H:1	Ductile confined masonry walls, one, two, and three stories	1230	1.62	796.62
MCF/LWAL/DUC/H:2		1736	2.29	1124.65
MCF/LWAL/DUC/H:3		651	0.86	421.74
MR/LWAL/DUC/H:1	Ductile reinforced masonry walls, one, two, and three stories	473	0.62	384.56
MR/LWAL/DUC/H:2		668	0.88	542.91
MR/LWAL/DUC/H:3		251	0.33	203.59
MUR/LWAL/DNO/H:1	Non-ductile unreinforced masonry walls, one, two, and three stories	14 738	19.45	3516.93
MUR/LWAL/DNO/H:2		19 682	25.97	4753.33
MUR/LWAL/DNO/H:3		7384	9.74	1783.33
MUR-ADO/LWAL/DNO/H:1	Non-ductile unreinforced masonry with adobe blocks walls, one and two stories	231	0.30	48.17
MUR-ADO/LWAL/DNO/H:2		254	0.34	54.71
MUR-STDRE/LWAL/DNO/H:1	Non-ductile unreinforced masonry with dressed stone walls, one and two stories	675	0.89	134.67
MUR-STDRE/LWAL/DNO/H:2		941	1.24	187.74
MUR-STRUB/LWAL/DNO/H:1	Non-ductile unreinforced masonry with semi-dressed stone, one and two stories	210	0.28	40.19
MUR-STRUB/LWAL/DNO/H:2		292	0.39	56.02
W/WLI/DUC/H:1	Ductile light wood members, one and two stories	1515	2.00	357.22
W/WLI/DUC/H:2		2246	2.96	554.13

group of variables, is one of the most common methods to objectively assess SV (Freudenberg, 2003). There are several methodological approaches for the construction of composite indicators, but in general, the steps include (1) the identification of pertinent variables, (2) the aggregation of variables into indicators and composite indicators, (3) multivariate analysis, (4) weighting, (5) convolution or link of variables, and (6) visualization and dissemination of results (Burton and Silva, 2016).

The SVI index aims to identify those municipalities in Sabana Centro whose inhabitants are more vulnerable to an earthquake based on a selection of specific variables, indicators, and composite indicators. The indicators were aggregated into five composite indicators constructed for the SVI of the SARA project (https://sara.openquake.org/development_of_indicators_of_social_vulnerability, last access: 12 January 2023): population, economy, infrastructure, education, and health. The composite indicator of the pop-

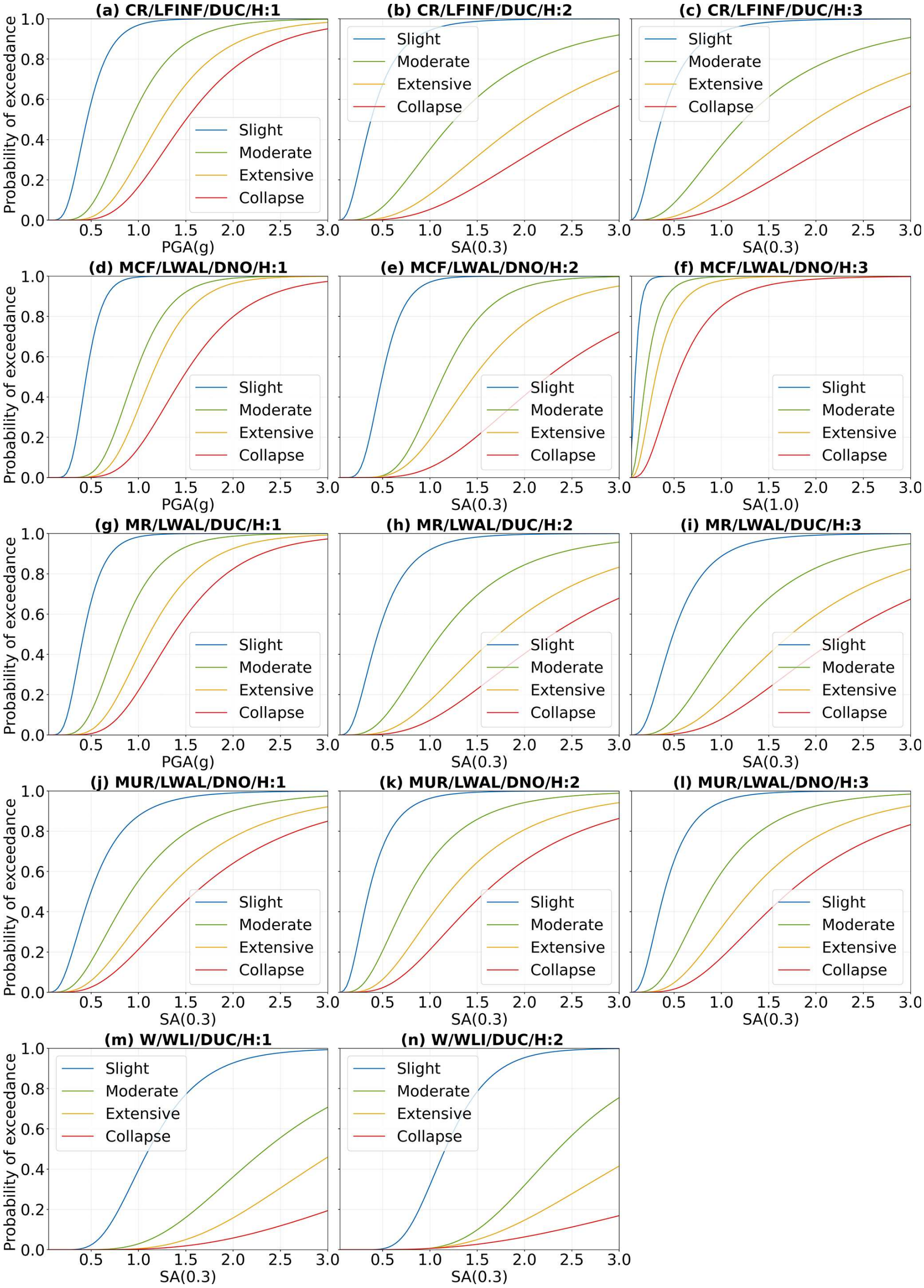

Figure 10. Fragility curves for 14 of the 33 building classes listed in Table 4. The curves describe the differential seismic vulnerabilities for the predominant building classes for each type of material: reinforced concrete (CR), confined masonry (MCF), reinforced masonry (MR), unreinforced masonry (MUR), and wood (W).

ulation considers the indicators that capture the capacity of the population to mitigate their risk and recover from earthquakes. In the current research the composite indicator of the population accounted initially for the female and native indigenous population, age dependence, population density, number of households, and people per household. The composite indicator of the economy includes indicators to assess the economic health of the community (Burton and Silva, 2016). The single indicators considered for this composite indicator were population unemployed, looking for employment, unsatisfied basic needs (UBNs), and impoverished. Poverty is an important aspect to consider because of its direct association with access to resources, which affects coping with the impacts of disasters (Fatemi et al., 2017). The composite indicator of infrastructure considers the access to basic services (Contreras et al., 2020b). The composite indi-

Table 5. Variance inflation factors (VIFs).

Coefficients[*]						
Model		Unstandardized coefficients		Standardized coefficients	Collinearity statistics	
		B	SE	Beta	Tolerance	VIF
1	(Constant)	0.728	0.000			
	Indigenous population	1.178	0.000	0.124	0.047	21.282
	Population density (inhabitants km^{-2})	−3.327	0.000	−0.047	0.030	33.453
	Number of people per household	−3.378	0.000	−0.012	0.029	34.994
	Population unemployed	10.076	0.000	0.134	0.191	5.222
	Population with unsatisfied basic needs	−8.921	0.000	−0.099	0.023	43.108
	Total population in poverty	7.205	0.000	0.129	0.238	4.203
	Households with no electric energy access	4.234	0.000	0.153	0.078	12.894
	No sewage system	1.160	0.000	0.123	0.351	2.848
	Illiteracy rate	−1.619	0.000	−0.027	0.209	4.785
	Deceased due to COVID-19	11.379	0.000	0.710	0.044	22.967

[*] Dependent variable: SV.

Table 6. Excluded variables.

Excluded variables[a]				
Model		Beta in	Collinearity statistics	
			Tolerance	Minimum tolerance
1	Female population	[b]	0.000	0.000
	Age dependence	[b]	0.000	0.000
	Total population	[b]	0.000	0.000
	Number of households	[b]	0.000	0.000
	Population looking for employment	[b]	0.000	0.000
	Households with a computer and internet	[b]	0.000	0.000
	Households with access to improved water source	[b]	0.000	0.000
	Education level completed: primary	[b]	0.000	0.000
	Education level: secondary	[b]	0.000	0.000
	Population enrolled in educational institution	[b]	0.000	0.000
	Hospital, clinics per 1000 population	[b]	0.000	0.000
	Population with no healthcare	[b]	0.000	0.000
	Population registered to national healthcare	[b]	0.000	0.000
	COVID-19 cases confirmed	[b]	0.000	0.000
	COVID-19 cases active	[b]	0.000	0.000
	People recovered from COVID-19	[b]	0.000	0.000

[a] Dependent variable: SV. [b] Predictors in the model: (constant), people dead due to COVID-19, total population in poverty, no sewage system, number of people per household, native indigenous population, population unemployed, illiteracy rate, population density (inhabitants km^{-2}), households with no electric energy access, and population with unsatisfied basic needs.

cator of education links the educational level and the socioeconomic status, mitigation, and recovery potential (Burton and Silva, 2016). It is assumed that a lower education level results in lower income, poor ability to understand emergencies, and a low capacity to recover after a disaster (Cutter et al., 2003). The composite indicator of health includes the indicators related to access to health facilities and healthcare (Contreras et al., 2020b). The lack of access to healthcare increases people's susceptibility to the potential impact of disasters (Fatemi et al., 2017). Considering the aforementioned composite indicators and the availability of information for the region, a total of 26 indicators were selected initially.

However, to avoid problems with interpreting the model and overfitting, we checked the multicollinearity by looking at the variance inflation factor (VIF) of each variable and indicator (see Table 5). The VIF was identified in a linear regression that included collinearity diagnostics produced in SPSS statistical software (Field, 2005). We excluded the variables and indicators that were potentially correlated with others and those that did not add significant information according to the collinearity diagnostics (Table 6). Eventually, the model included 10 independent and relevant variables and indicators to estimate the SV in the case study area (Table 7).

Much of the information used for the indicators is from the national census (DANE, 2018) database; studies such as the multipurpose survey (EM2017), which examined the quality of life of households in Bogotá and surrounding areas (https://sdpbogota.maps.arcgis.com/apps/MapJournal/index.html?appid=c984e588b0764efbb424ffc2207b5cf6, last access: 23 December 2022); and the analysis of the characteristics of the population in Sabana Centro (Sabana Centro Cómo Vamos, 2019).

The min–max normalization was used to standardize the SV indicators from zero to one to estimate the SVI per municipality. Higher scores indicate more socially vulnerable municipalities, and lower scores reflect less vulnerable ones. Then, the indicators were integrated by summing them with equal weight, as followed in Contreras et al. (2020c). The resulting SVI index is therefore used to adjust the percentage of economic losses with respect to the costs presented by the building inventory, i.e., multiplying them by $1 + \mathrm{SVI}$ (Carreño et al., 2007).

4 Results

This section presents the results of this study in terms of median building damage and median economic losses for each municipality. First, the M_w 5.95 earthquake scenario results in Chía are introduced to illustrate the methodology. Then, the results of the 18 seismic risk scenarios for Sabana Centro are presented. These 18 scenarios are defined based on the earthquake events presented in Table 2. These did not include directivity effects because there was insufficient information available for a reliable model. The economic losses are adjusted based on the SVI discussed in Sect. 3.4 and are also presented. For this purpose, before presenting the economic losses, the SVI calculation will be introduced.

4.1 Damage forecast

The predicted damage for the M_w 5.95 earthquake scenario in Chía considered for the region is presented in Table 8. The mean and standard deviation are presented for each of the damage states considered in the scenario. The respective distribution of the ground motion field for the 5.95 earthquake is presented in Fig. 11.

In the region, 42.95 % of the buildings considered in the exposure model are expected to suffer some degree of damage. This result represents 32 598 out of the 75 778 analyzed buildings. Table 8 shows that the type of damage with the highest occurrence is slight (21.31 %), followed by collapse (9.85 %), moderate (7.36 %), and extensive damage (4.44 %). Overall, 14.28 % might suffer extensive or collapse damage; hence they will not fulfill their life safety functionality. Nearly 10 % of collapse raises concerns from a decision-maker perspective, but two Colombian events put the results in perspective: the M_w 6.1 earthquake in Armenia (1999) and the M_w 5.5 earthquake in Popayán (1983). In the former, the records indicate that 17 551 buildings were destroyed, 18 421 had severe damage, and 43 474 had moderate damage. In the latter, which occurred at an estimated depth between 12 and 15 km, 12 % of buildings suffered complete damage. In both earthquakes, damage concentrated in unreinforced masonry buildings, constructed prior to the enactment of the Colombian seismic design code in 1998. More than 60 % of the building stock in Sabana Centro is comprised of that type of building, and furthermore, 35 % are two- and three-story houses (Table 4), which are more vulnerable than one-story houses (Heresi and Miranda, 2022a). These buildings are expected to withstand significant damage during an earthquake such as the Chía M_w 5.95 shown here, which is similar in magnitude and depth to the Armenia earthquake and for which the percentage of collapse herein presented is similar to that from the Popayán earthquake.

In terms of municipalities, higher damage occurs in Chía and Cajicá, with 3522 and 2271 collapsed buildings. Compared to the total buildings of each municipality, collapses account for 19.0 % and 19.7 %, respectively. Overall, they account for 5793 out of the 7463 collapsed buildings for this scenario (77 %). In contrast, Cogua was the municipality with the lowest number of damaged buildings, as roughly 90 % of the inventory did not experience any type of damage, and only 0.33 % of them collapsed. Nemocón had the least damages after Cogua, with 2.4 % of collapses. These results are reasonable because Chía and Cajicá are closer to the epicenter in this scenario, and they have the highest building inventory of the region, together with Zipaquirá. Besides, a significant part of their building inventory is comprised of non-ductile unreinforced masonry. On the other hand, despite having a similar distribution of the building inventory, Cogua and Nemocón are the farthest municipalities from the epicenter. The main difference between these two is that Nemocón has softer soils, with roughly one-fourth of the municipality under $180\,\mathrm{m\,s^{-1}}$, thus the higher percentage of collapses.

The highest concentration of building collapses in the region is expected for houses constructed of unreinforced masonry (Table 9), mostly involving non-ductile unreinforced masonry walls of one and two stories (22.8 % and 30.5 %, respectively). Notably, these two types of buildings account for 53.30 % of collapses. Three-story unreinforced masonry houses account for 10.12 % of buildings, making the over-

Table 7. Selected variables.

Collinearity diagnostics*												
Model		1										
		1	2	3	4	5	6	7	8	9	10	11
Eigenvalue		8.495	1.004	0.740	0.517	0.102	0.066	0.044	0.017	0.011	0.004	4.453×10^{-5}
Condition index		1.000	2.909	3.389	4.053	9.134	11.307	13.893	22.300	27.201	48.357	436.754
Variance Proportions	(Constant)	0.00	0.00	0.00	0.00	0.00	0.00	0.00	0.00	0.00	0.00	1.00
	Native indigenous population	0.00	0.02	0.00	0.02	0.03	0.00	0.00	0.00	0.00	0.04	0.89
	Population density (inhabitants km^{-2})	0.00	0.00	0.00	0.00	0.00	0.00	0.00	0.01	0.00	0.24	0.74
	Number of people per household	0.00	0.00	0.00	0.00	0.00	0.00	0.00	0.00	0.00	0.00	1.00
	Population unemployed	0.00	0.00	0.00	0.00	0.00	0.03	0.00	0.21	0.00	0.75	0.00
	Population with unsatisfied basic needs	0.00	0.00	0.00	0.00	0.00	0.00	0.00	0.01	0.02	0.00	0.96
	Total population in poverty	0.00	0.00	0.00	0.00	0.01	0.15	0.10	0.01	0.12	0.45	0.16
	Households with no electric energy access	0.00	0.00	0.00	0.00	0.09	0.04	0.01	0.08	0.00	0.73	0.05
	No sewage system	0.00	0.08	0.15	0.13	0.00	0.02	0.01	0.07	0.03	0.08	0.42
	Illiteracy rate	0.00	0.00	0.00	0.00	0.01	0.02	0.16	0.01	0.32	0.02	0.47
	People dead due to COVID-19	0.00	0.00	0.01	0.02	0.04	0.00	0.00	0.11	0.03	0.08	0.71

* Dependent variable: SV.

all contribution of this structural system more than 6 out of 10 collapses. The percentage of three-story houses collapsed was smaller than the one from two-story houses (which are less vulnerable) because three-story houses are less frequent in the region.

The number of expected damaged buildings for each municipality due to the Chía M_w 5.95 scenario is presented in Fig. 12. It also shows their percentages for each damage state relative to the province's total. These results show that Chía, Cajicá, and Sopó have the highest percentage of collapsed buildings, with 47.20 %, 30.43 %, and 7.37 %, respectively. In this scenario, the least affected municipalities are Cogua and Nemocón, with less than 1 % of collapse percentages.

The damage calculations were conducted for all the seismic events presented in Table 2. Table 10 shows the resulting percentage of buildings that suffer damage for each of the 18 seismic risk scenarios. The results show that the worst scenario for the region is the M_w 6.95 in Cota, which has 21.37 % collapsed buildings, and the highest percentages of severe and moderate damage. Interestingly, the M_w 6.85 in Tocancipá had 8.12 % of collapsed buildings, roughly 2.5 times less than the M_w 6.95 in Cota. This difference is a consequence of the uneven distribution of the building stock in the region, as nearly 40 % is in Chía and Cajicá, which are close to Cota. A similar situation occurs for the earthquakes of M_w 6.25 in Sopó, Tabio, and Cajicá.

Figure 13 shows the variability of the results for each damage state of Table 10. The results illustrate the notable variability of the damage estimates between the different seismic scenarios. This variability is higher for the no-damage state, which ranges between 32.49 % and 76.99 %, corresponding to the M_w 6.95 in Cota and the M_w 5.35 in Tenjo scenarios. These two also had the highest and lowest percent of collapse, respectively. The median results of the 18 scenarios for the damage states are 53.6 %, 24.1 %, 8.1 %, 4.7 %, and 9.5 %, values that are close to those of the M_w 6.25 in Tabio.

4.2 Social vulnerability index (SVI)

According to the methodology presented in Sect. 3.4, the SVI is calculated and shown in Table 11.

Table 8. Number and percentage of buildings expected to suffer damage in the region after the M_w 5.95 earthquake scenario in Chía. The mean and standard deviation (SD) for each of the GMPE and damage states are presented.

Municipality	GMPE	No damage		Slight		Moderate		Extensive		Collapse	
		Mean	SD	Mean	SD	Mean	SD	Mean	SD	Mean	SD
Cajicá	Abrahamson	5520	904	3700	420	1133	298	560	193	590	332
	Cauzzi	2745	1067	3015	727	1486	347	1084	268	3176	1270
	Mean*	3716		3255		1362		901		2271	
Chía	Abrahamson	9173	1493	5809	689	1773	486	872	311	916	545
	Cauzzi	4817	1779	4870	1170	2285	568	1645	427	4926	2084
	Mean*	6342		5199		2105		1374		3522	
Cogua	Abrahamson	2688	209	257	148	38	42	13	18	9	24
	Cauzzi	2712	211	233	147	37	43	13	20	10	28
	Mean*	2704		241		37		13		10	
Cota	Abrahamson	3175	484	932	264	233	124	103	70	120	145
	Cauzzi	3313	508	817	284	206	121	99	71	128	168
	Mean*	3264		858		216		100		126	
Gachancipá	Abrahamson	1777	232	519	134	116	60	47	31	40	42
	Cauzzi	1637	289	530	153	152	74	77	45	103	101
	Mean*	1686		526		140		66		81	
Nemocón	Abrahamson	1408	164	337	102	66	40	25	19	18	21
	Cauzzi	1282	212	364	113	99	54	49	32	60	64
	Mean*	1326		355		88		41		45	
Sopó	Abrahamson	1258	341	1116	197	476	101	290	81	520	269
	Cauzzi	1403	428	1009	220	414	115	267	88	566	319
	Mean*	1352		1047		436		275		550	
Tabio	Abrahamson	1745	319	775	159	225	89	108	56	135	122
	Cauzzi	1918	346	668	180	185	89	93	55	124	126
	Mean*	1858		705		199		98		128	
Tenjo	Abrahamson	1976	248	627	140	142	67	58	35	48	44
	Cauzzi	1678	330	657	165	210	84	117	56	189	156
	Mean*	1782		647		186		96		140	
Tocancipá	Abrahamson	2807	463	1443	222	406	141	187	86	189	147
	Cauzzi	2196	593	1361	303	513	159	317	118	646	418
	Mean*	2410		1390		475		272		486	
Zipaquirá	Abrahamson	16 638	1568	2067	1048	349	341	125	155	98	207
	Cauzzi	16 873	1589	1847	1047	326	344	124	164	108	247
	Mean*	16 791		1924		334		125		105	
Total	Number of buildings	43 230		16 145		5579		3361		7463	
	Percentage of buildings (%)	57.05		21.31		7.36		4.44		9.85	

The mean * is calculated with the corresponding weights for each GMPE (Abrahamson et al., 2014: 0.35, and Cauzzi et al., 2014: 0.65). The total number and percentage of buildings for each damage state are at the end of the table.

Considering population, the most vulnerable municipality is Cota and the least vulnerable is Tenjo. Regarding economy, the most vulnerable is Gachancipá and the least vulnerable is Tabio. In the case of infrastructure, the most vulnerable municipality is Cajicá and the least vulnerable is Gachancipá. In terms of education, the municipality of Cogua is the most vulnerable, followed by Nemocón, unlike Chía. The health composite indicator shows that Zipaquirá is the most vulnerable municipality and the least vulnerable is Gachancipá. The economy composite indicator shows higher vulnerability indices than the other categories for most municipalities. Evaluating all of the categories, it was found that Zipaquirá is the municipality with the highest SVI, while Tabio is the least vulnerable.

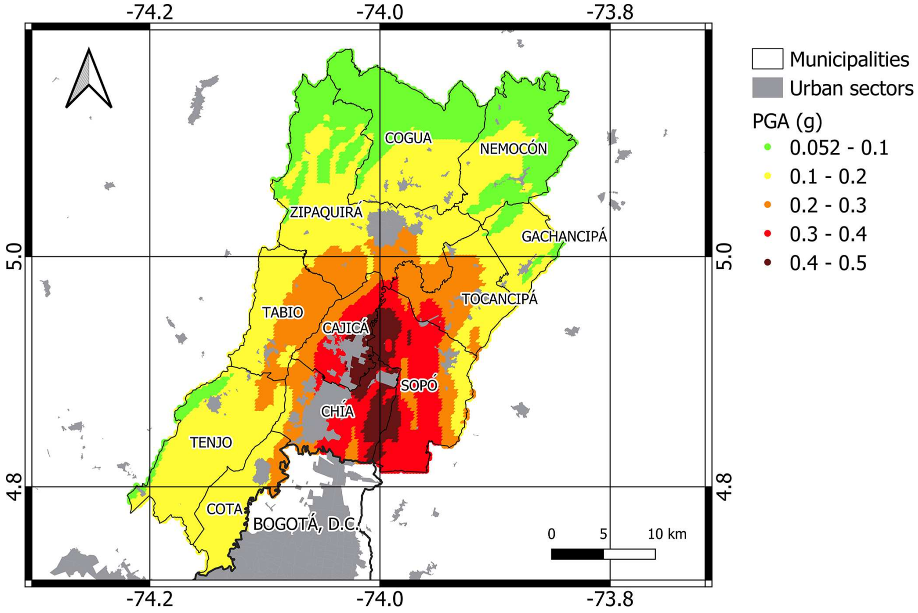

Figure 11. Estimated maximum peak ground acceleration (PGA) in bedrock for the M_w 5.95 Chía earthquake. The highest acceleration is presented in dark red and the lowest in green.

4.3 Economic losses from the M_w 5.95 Chía earthquake scenario

The direct total economic loss arising from the considered M_w 5.95 Chía scenario is USD 900.49 million, which represents 14.41 % of the total replacement cost of the building inventory. The municipalities that contribute the most to these losses are Chía, with 52.60 %, and Cajicá, with 23.97 %, as shown in Table 12. This result was expected, since these municipalities' urban growth is high compared to the other municipalities. The smallest contribution comes from Cogua and Nemocón, with 0.06 % and 0.18 %, respectively. Overall, in the case of this M_w 5.95 earthquake scenario, the direct economic loss in terms of replacement costs would be approximately 21 % of the region's GDP. The economic losses for each municipality are presented in Table 12 and Fig. 14a. Cajicá is the one with the highest percentage of losses, with 22.66 % of the replacement costs. Other municipalities for which high economic losses are expected are Chía and Sopó, with 21.71 % and 17.22 %, respectively. The municipalities with the lowest losses are Zipaquirá (0.93 %) and Cogua (0.67 %).

Figure 14b shows the adjusted economic losses by municipality and includes SV. After considering the SV in the region, the economic losses increase by 27.42 %, from USD 900.49 to 1240.72 million. The municipality that would have the highest economic losses is Cajicá (22.66 % of the building replacement cost), with USD 215.80 million. When the SV is included, its potential economic losses increase to USD 306.61 million (32.19 % of the replacement cost of Cajicá buildings). In the case of Zipaquirá, the most socially vulnerable municipality, the losses were initially USD 5.08 million and increase to USD 7.85 million when the SVI is accounted for.

The percentage of economic losses concerning the building types relative to the total losses in the region is shown in Table 13. A total of 41 % of losses come from unreinforced masonry buildings (MUR/LWAL/DNO/H1 and MUR/LWAL/DNO/H2). This result is expected because this building type has a high seismic vulnerability, while the lowest contribution would come from CR/LDUAL/-DUC/H:4,7 houses, with less than 0.02 %. Three-story non-ductile houses constructed in reinforced concrete frames and confined masonry experienced the highest collapsed buildings per taxonomy, with nearly 20 % for both. In the case of the frames, 18.63 % of two-story houses collapsed, more than twice of those of one story. In the case of non-ductile confined masonry this ratio was 5, while for ductile confined masonry it was 4. These results agree with the findings by Heresi and Miranda (2022a) and add evidence to the need of avoiding lumping low-rise houses (one to three stories) into a single taxonomy for seismic risk calculations.

4.4 Mean direct economic losses for the earthquake scenarios

The seismic ground motion fields expected for each earthquake scenario listed in Table 2 were simulated 1000 times to account for their aleatoric uncertainty as advised by Silva (2016), making use of the OQ Engine. The physical vulnerability was calculated in a similar manner as for the M_w 5.95 earthquake scenario. Figure 15 shows the loss-

Table 9. Expected number and percentage of buildings by class that might collapse as a result of the M_w 5.95 earthquake scenario in Chía and their corresponding economic losses presented in millions of USD and as a percentage of total losses.

Building classes	Number of collapsed buildings	Percentage out of the collapsed buildings (%)	Direct economic losses (USD in millions)	Percentage out of the economic losses (%)
CR/LDUAL/DUC/H:4,7	2	0.02	1.49	0.17
CR/LFINF/DUC/H:1	24	0.32	6.77	0.75
CR/LFINF/DUC/H:2	68	0.91	19.74	2.19
CR/LFINF/DUC/H:3	27	0.36	7.88	0.87
CR/LFINF/DUC/H:4,7	42	0.56	45.24	5.02
CR/LFM/DNO/H:1	77	1.03	18.17	2.02
CR/LFM/DNO/H:2	225	3.01	53.28	5.92
CR/LFM/DNO/H:3	89	1.19	21.12	2.35
CR/LFM/DUC/H:4,7	31	0.42	33.13	3.68
CR/LWAL/DUC/H:4,7	10	0.14	11.81	1.31
CR/LWAL/DUC/H:1	1	0.02	0.63	0.07
CR/LWAL/DUC/H:2	9	0.12	3.79	0.42
CR/LWAL/DUC/H:3	3	0.04	1.27	0.14
MCF/LWAL/DNO/H:1	156	2.09	16.05	1.78
MCF/LWAL/DNO/H:2	868	11.63	51.23	5.69
MCF/LWAL/DNO/H:3	513	6.88	53.45	5.94
MCF/LWAL/DUC/H:1	17	0.23	5.02	0.56
MCF/LWAL/DUC/H:2	93	1.24	25.95	2.88
MCF/LWAL/DUC/H:3	42	0.56	11.61	1.29
MR/LWAL/DUC/H:1	16	0.21	5.56	0.62
MR/LWAL/DUC/H:2	45	0.6	15.98	1.77
MR/LWAL/DUC/H:3	17	0.23	5.99	0.67
MUR/LWAL/DNO/H:1	1702	22.8	155.82	17.3
MUR/LWAL/DNO/H:2	2276	30.5	223.88	24.86
MUR/LWAL/DNO/H:3	755	10.12	75.51	8.39
MUR-ADO/LWAL/DNO/H:1	33	0.45	2.6	0.29
MUR-ADO/LWAL/DNO/H:2	32	0.43	2.73	0.3
MUR-STDRE/LWAL/DNO/H:1	75	1.01	5.84	0.65
MUR-STDRE/LWAL/DNO/H:2	105	1.41	8.65	0.96
MUR-STRUB/LWAL/DNO/H:1	22	0.3	1.8	0.2
MUR-STRUB/LWAL/DNO/H:2	30	0.4	2.47	0.27
W/WLI/DUC/H:1	24	0.32	2.44	0.27
W/WLI/DUC/H:2	33	0.44	3.61	0.4
Total	7463	100	900.49	100

exceedance curves that describe the probability of exceeding a given percent of economic losses for each earthquake scenario.

Among the simulated scenarios, the most significant economic losses might occur with the scenario that considers an earthquake of M_w 6.95 in Cota and the smallest with the simulation of the earthquake of M_w 5.35 in Tenjo. For example, the probability that economic losses exceed 20 % in the 6.95 Cota scenario is 61 %, while for the scenario 5.35 in Tenjo, the probability is 3 %. Besides magnitude, the uneven distribution of the building stock in the region is an important factor that exerts an influence on economic losses, as shown by the differences between the three M_w 6.25 events in Fig. 15. The highest economic losses are in the municipality of Cota with 24.29 % of losses (USD 1517.56 million). On average, economic losses when including social vulnerability increase by 37 % as shown in Table 14.

5 Discussion

5.1 Damage and losses

The findings presented in this work show that the Sabana Centro province is exposed to a considerable level of seismic risk. The simulations of 18 seismic scenarios with a return period of 475 years extracted from a probabilistic seismic hazard assessment (PSHA) show that the damaged buildings ranged between 23 % and 67.5 % of the building stock depending on the earthquake epicenter. Worryingly, the median value of buildings that would experience extensive damage

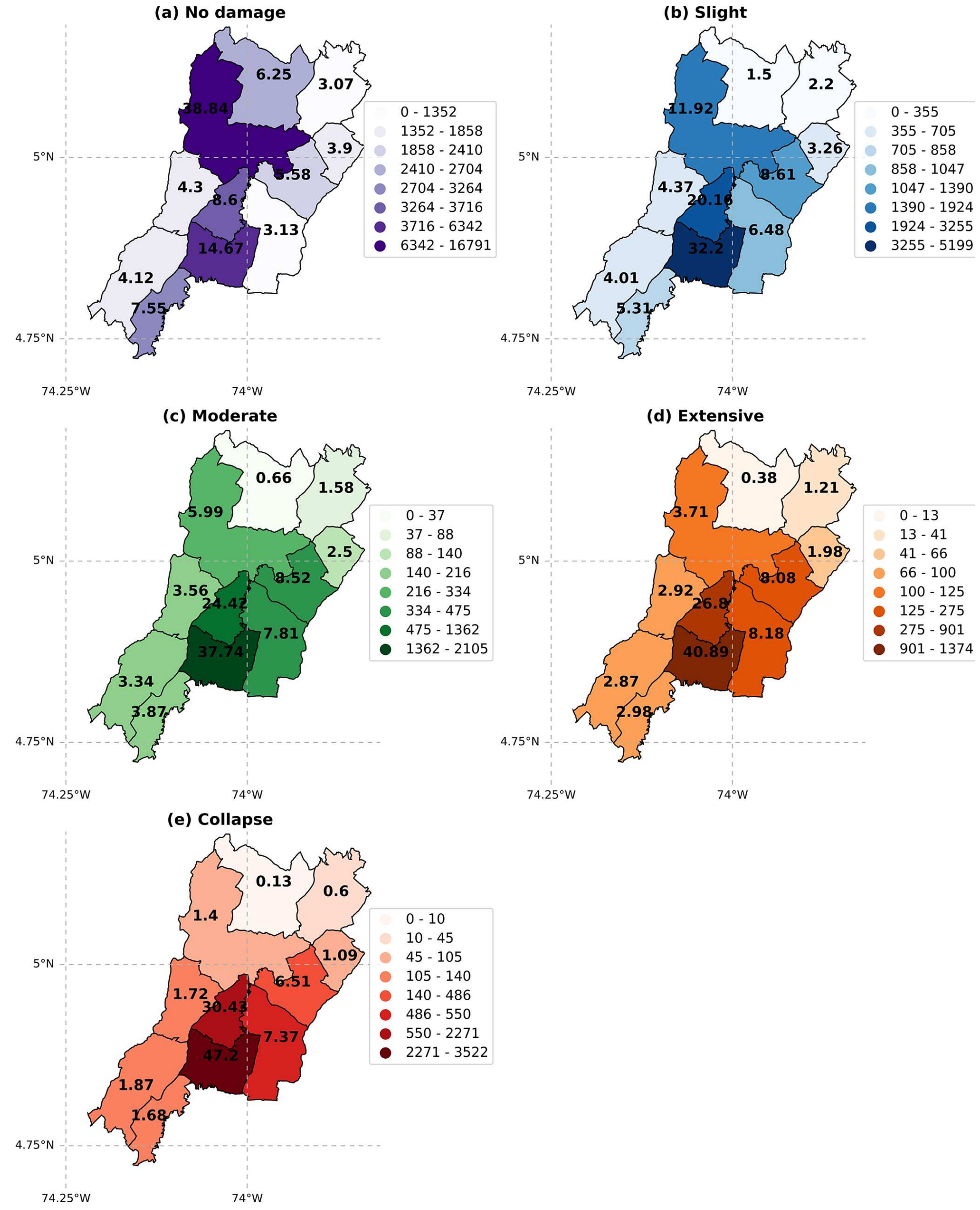

Figure 12. Number of buildings expected to experience **(a)** no damage, **(b)** slight damage, **(c)** moderate damage, **(d)** extensive damage, or **(e)** collapse as a result of the M_w 5.95 earthquake scenario in Chía. The corresponding percentage values of buildings are presented within each municipality.

or collapse in the 18 scenarios is 14.2 %. This situation stems from the fact that 83 % of the houses in the province are constructed using non-ductile structural systems. These houses accounted for more than 90 % of collapses in most of the scenarios. The damage results also highlight the importance of discretizing buildings with the same structural system by height, at least for houses between one and three stories as suggested by Heresi and Miranda (2022a) because two- and three-story houses had a significantly higher percentage of collapses compared to one-story houses.

In terms of economic losses, the median expected cost of the 18 earthquakes selected from the PSHA in the province is 19 % of its GDP, which accounts for USD 809.46 million, almost 13 % of the replacement cost of the building inventory. This result only accounts for the cost of physical damage of the building stock, however, and does not represent all of the potential impacts.

Table 10. Expected damage for each of the 18 scenarios presented in Table 2. The name of the scenarios has the magnitude of the events and the municipality where they are located.

Scenario	Percentage of buildings for each damage state				
	No damage	Slight	Moderate	Extensive	Collapse
5.35 Tenjo	76.99	14.41	3.86	1.95	2.79
5.55 Cota	74.44	15.17	4.35	2.32	3.72
5.65 Zipaquirá	62.77	22.12	6.48	3.41	5.23
5.95 Chía	57.05	21.31	7.36	4.44	9.85
5.95 Gachancipá	66.78	19.60	5.66	3.01	4.94
5.95 Tenjo	73.69	15.72	4.41	2.35	3.83
6.15 Tocancipá	63.26	20.44	6.25	3.49	6.56
6.25 Nemocón	65.26	19.73	5.81	3.19	6.01
6.25 Sopó	44.90	25.57	9.48	5.90	14.14
6.25 Tabio	54.11	24.11	8.02	4.64	9.12
6.35 Cajicá	38.73	26.89	10.63	6.83	16.92
6.35 Cogua	47.20	26.56	9.49	5.66	11.09
6.45 Cogua	39.74	27.14	10.61	6.74	15.77
6.55 Sopó	35.51	26.97	11.08	7.29	19.15
6.65 Nemocón	51.80	24.04	8.29	4.95	10.92
6.65 Tabio	42.97	25.86	9.84	6.23	15.10
6.85 Tocancipá	53.10	25.37	8.57	4.84	8.12
6.95 Cota	32.49	26.86	11.51	7.78	21.37

Table 11. SVI for the municipalities of the Sabana Centro province.

Composite indicators	Municipalities										
	Cajicá	Chía	Cogua	Cota	Gachancipá	Nemocón	Sopó	Tabio	Tenjo	Tocancipá	Zipaquirá
Population	0.47	0.30	0.62	0.69	0.57	0.32	0.36	0.31	0.00	0.46	0.68
Economy	0.56	0.50	0.42	0.57	0.83	0.56	0.31	0.06	0.54	0.66	0.49
Infrastructure	0.69	0.50	0.13	0.25	0.00	0.11	0.01	0.05	0.09	0.14	0.269
Education	0.06	0.00	1.00	0.26	0.41	0.96	0.28	0.33	0.26	0.27	0.28
Health	0.33	0.70	0.09	0.06	0.00	0.03	0.08	0.03	0.05	0.15	1.00
Index	0.42	0.40	0.45	0.37	0.36	0.40	0.21	0.16	0.19	0.34	0.54

5.2 Effects of social vulnerability (SV)

Very few research studies have tested the correlation between social vulnerability (SV) and losses. To the best of our knowledge, the relationship between SV and modeled losses has so far been informative rather than indicating that total losses (measured as dollar losses or debris generated) increase with SV (Schmidtlein et al., 2011). However, it was found that only relative losses (dollar losses per average family income) tend to increase with SV. Case study areas with a low SV tend to have more material goods with significant monetary value (dollar) exposed to risk than areas with high SV. Therefore, we should expect a negative correlation between property losses and SV (Cutter and Finch, 2008). It is important to understand that while the total loss (dollar) in case study areas with high SV is lower, the impact of those losses in their communities is high (Schmidtlein et al., 2011). Integrating the level of SV to the physical losses will not produce a significant increase in the last ones, considering that they are negatively correlated (Cutter and Finch, 2008), but the result will be a more holistic risk assessment, also useful to prioritize actions at the regional level. Sabana Centro is a province with a significant level of SV, representing many areas in Colombia and other countries in South America, with essential deficiencies in areas like health and education. The estimated integration of SV with the economic losses increases them to 26 % of the GDP, representing approximately USD 1.11 billion. The results of this study show that including SV is important in risk analysis, as it allows one to go beyond only considering economic loss assessments with respect to physical damage.

5.3 Caveats and limitations

There are several limitations that should be addressed in future studies. One of them involves the selection of the

Table 12. Economic losses for the region as a result of the considered M_w 5.95 earthquake scenario. Economic losses with SV consider the percentage of losses with respect to the total losses per municipality and are adjusted using the SVI. Consequently, the losses in millions of USD are adjusted.

Municipality	Cost of building inventory	Direct economic losses			Economic losses with social vulnerability	
	(USD in millions)	Losses (USD in millions)	Losses with respect to the total (%)	Percentage of municipality cost (%)	Losses + SVI (%)	Losses after considering the SVI (USD in millions)
Cajicá	952.41	215.80	23.97	22.66	32.19	306.61
Chía	2182.19	473.68	52.60	21.71	30.38	662.98
Cogua	87.74	0.58	0.06	0.67	0.97	0.85
Cota	646.16	24.19	2.69	3.74	5.11	33.03
Gachancipá	49.94	2.37	0.26	4.74	6.46	3.22
Nemocón	42.82	1.62	0.18	3.77	5.27	2.25
Sopó	252.55	43.48	4.83	17.22	20.81	52.56
Tabio	205.93	11.60	1.29	5.63	6.52	13.42
Tenjo	539.13	35.14	3.90	6.52	7.74	41.74
Tocancipá	742.61	86.95	9.66	11.71	15.65	116.21
Zipaquirá	547.03	5.08	0.56	0.93	1.43	7.85
Total	6248.51	900.49	100.00			1240.72

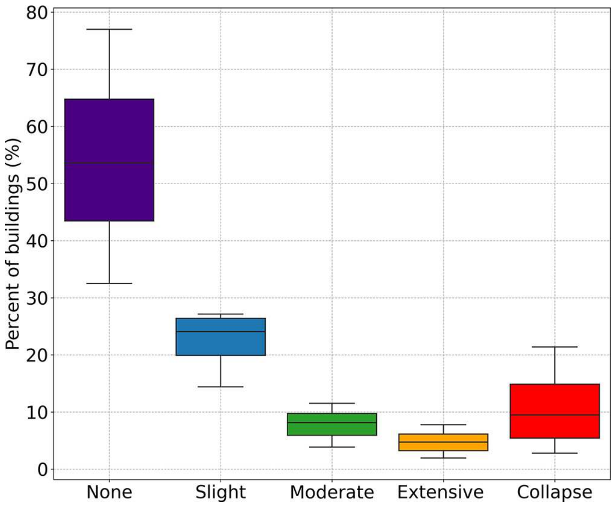

Figure 13. Percent of buildings expected to experience no damage ("none"), slight damage, moderate damage, extensive damage, or collapse as a result of the 18 earthquake scenarios presented in Table 2.

building's seismic fragility functions. Recent research has demonstrated that assumptions about several input parameters used in physical seismic vulnerability significantly influence risk assessment in urban areas (Hoyos and Hernández, 2021). One concern held by the authors is that the field observations and surveys show that a big part of the building stock of Sabana Centro is the result of informal construction. Presently, these buildings are constructed using either confined masonry or infilled RC frames due to the influence of the Colombian design code (which has similarities to the ACI-318; Arroyo et al., 2019), which forbade unreinforced masonry. Research about fragility functions like these buildings in Puerto Rico (Murray et al., 2022) and Villavicencio (Feliciano et al., 2022) shows that the collapse probability may be even twice more than that of code-conforming buildings. The fragility functions by Martins and Silva (2021) and Villar-Vega (2017) used in this research do not account for the particularities of these buildings; thus the authors hold the hypothesis that the damage estimates should be considered a lower bound.

It is important to mention that the exposure model for residential buildings developed in this study considered two types of exposure modeling approaches. On the one hand, the census-based part is a top-down approach from aggregated data. On the other hand, the rapid remote surveys constitute a bottom-up approach. Although the latter allowed an assessment of the validity of the assumed building classes, both approaches were not fully integrated through a probabilistic approach (Pittore et al., 2020). Although this method requires more computational efforts, it is worth exploring in future studies.

Another aspect that was not explicitly addressed in this study was the consideration of spatial cross-correlation models in modeling the ground motion fields. Several studies (e.g., Weatherill et al., 2015; Heresi and Miranda, 2022b) have demonstrated the relevance of such models in seismic risk assessment for building portfolios when sets of fragility functions that consider several intensity measures (IMs) are implemented. Although when such models are accommodated, the loss outcomes typically show a greater dispersion

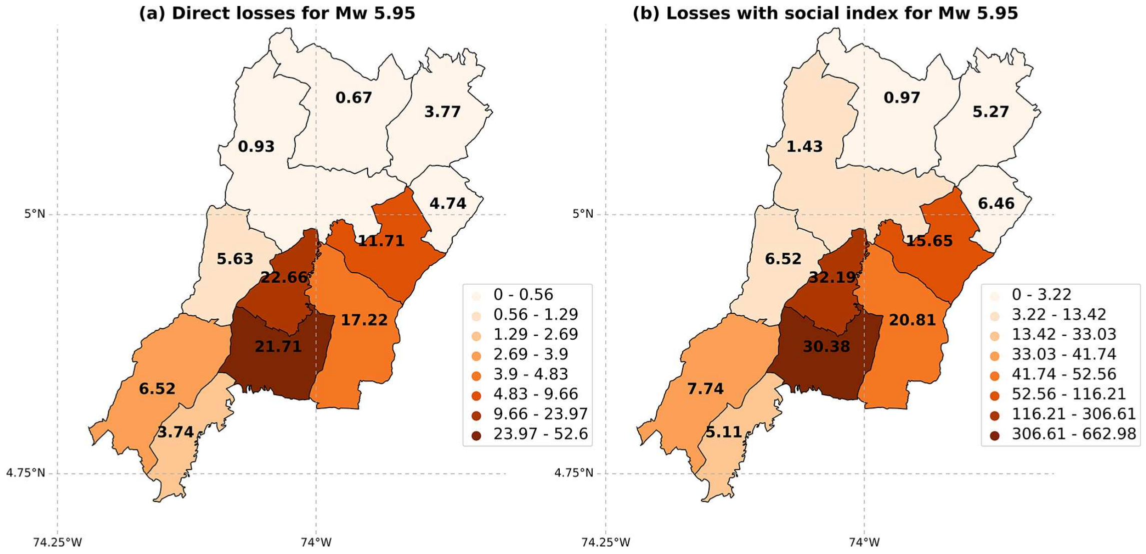

Figure 14. **(a)** Expected losses in millions of US dollars for the region as a result of the M_w 5.95 earthquake scenario and **(b)** the expected losses after considering the SVI. The percentage of losses with respect to the total is presented within the municipalities.

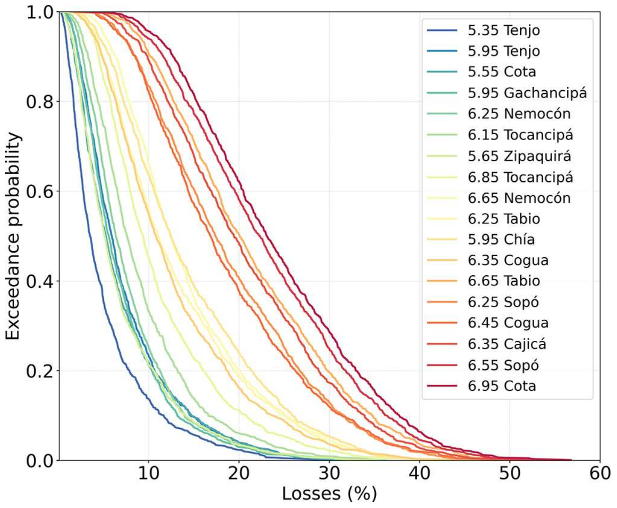

Figure 15. Loss-exceedance curves (LECs) as a function of the percentage of economic losses in the region for the 18 earthquake scenarios considered (Table 2) whose ground motion fields were simulated 1000 times. The legend is sorted according to the line position in the figure from left to right.

(and are more likely to give extreme values), while when such models are disregarded, the mean loss values forecasted have been observed to be practically the same as for the cases when a spatial correlation model was used (e.g., Michel et al., 2017; Gomez-Zapata et al., 2021). Therefore, the results presented in this study are still informative, but once again, we remark they should be treated as lower bounds for the considered risk scenarios.

Furthermore, due to the proximity of the study area to the Usme fault, near-fault effects might be expected. Hence, the study of possible directivity effects might be relevant for future studies. The evaluation of this feature has been shown to be relevant in both seismic ground motion (Türker et al., 2022) and earthquake loss models (Gentile and Galasso, 2021). Therefore, a better understanding of their role in risk scenarios will benefit the outlined results.

Another point is that this study did not consider human casualties. These were not included due to the lack of accurate information about housing occupation, since in this province, it is expected that more than one family share one dwelling. Notwithstanding, the median results of physical damage assessment for the 18 scenarios suggest that 14.2 % of buildings will have a seismic performance below the life safety level. The limited number and quality condition of hospitals and healthcare facilities in the province would further exacerbate the potential impact of an earthquake on the population.

6 Conclusions and future work

This paper presented the results of a seismic risk assessment for the Sabana Centro province in Colombia, which also accounted for the effects of SV. A total of 18 earthquake scenarios with a return period of 475 years were selected from a hazard disaggregation study. Each scenario was simulated 1000 times using the OQ Engine to calculate the physical damage and economic losses. These were adjusted based on an SVI that included the effects of the ongoing COVID-19 pandemic. The key findings from the results of this study are as follows:

- Sabana Centro is a region in a high-seismic-risk area. A total of 10 % of the buildings would collapse and 4.44 % would experience extensive damage considering

Table 13. Expected number and percentage of buildings by class that might collapse as a result of the M_w 5.95 earthquake scenario in Chía and their respective economic losses.

Building class	Number of collapsed buildings	Percentage of buildings (%)	Percentage of collapsed buildings by taxonomy (%)	Economic losses (USD in millions)	Percentage out of the economic losses (%)
CR/LDUAL/DUC/H:4,7	2	0.02	11.63	1.49	0.17
CR/LFINF/DUC/H:1	24	0.32	2.81	6.77	0.75
CR/LFINF/DUC/H:2	68	0.91	5.61	19.74	2.19
CR/LFINF/DUC/H:3	27	0.36	5.98	7.88	0.87
CR/LFINF/DUC/H:4,7	42	0.56	8.96	45.24	5.02
CR/LFM/DNO/H:1	77	1.03	9.01	18.17	2.02
CR/LFM/DNO/H:2	225	3.01	18.63	53.28	5.92
CR/LFM/DNO/H:3	89	1.19	19.67	21.12	2.35
CR/LFM/DUC/H:4,7	31	0.42	6.74	33.13	3.68
CR/LWAL/DUC/H:4,7	10	0.14	3.53	11.81	1.31
CR/LWAL/DUC/H:1	1	0.02	0.72	0.63	0.07
CR/LWAL/DUC/H:2	9	0.12	3.86	3.79	0.42
CR/LWAL/DUC/H:3	3	0.04	3.51	1.27	0.14
MCF/LWAL/DNO/H:1	156	2.09	2.53	16.05	1.78
MCF/LWAL/DNO/H:2	868	11.63	12.31	51.23	5.69
MCF/LWAL/DNO/H:3	513	6.88	19.40	53.45	5.94
MCF/LWAL/DUC/H:1	17	0.23	1.40	5.02	0.56
MCF/LWAL/DUC/H:2	93	1.24	5.33	25.95	2.88
MCF/LWAL/DUC/H:3	42	0.56	6.46	11.61	1.29
MR/LWAL/DUC/H:1	16	0.21	3.34	5.56	0.62
MR/LWAL/DUC/H:2	45	0.60	6.74	15.98	1.77
MR/LWAL/DUC/H:3	17	0.23	6.91	5.99	0.67
MUR/LWAL/DNO/H:1	1702	22.80	11.55	155.82	17.30
MUR/LWAL/DNO/H:2	2276	30.50	11.56	223.88	24.86
MUR/LWAL/DNO/H:3	755	10.12	10.23	75.51	8.39
MUR-ADO/LWAL/DNO/H:1	33	0.45	14.41	2.60	0.29
MUR-ADO/LWAL/DNO/H:2	32	0.43	12.70	2.73	0.30
MUR-STDRE/LWAL/DNO/H:1	75	1.01	11.14	5.84	0.65
MUR-STDRE/LWAL/DNO/H:2	105	1.41	11.18	8.65	0.96
MUR-STRUB/LWAL/DNO/H:1	22	0.30	10.71	1.80	0.20
MUR-STRUB/LWAL/DNO/H:2	30	0.40	10.19	2.47	0.27
W/WLI/DUC/H:1	24	0.32	1.57	2.44	0.27
W/WLI/DUC/H:2	33	0.44	1.47	3.61	0.40
Total	7463	100.00		900.49	100.00

the 5.95 M_w Chía scenario. The damage is concentrated on non-ductile unreinforced masonry houses, which account for 63.4 % of the building stock. The most significant contribution to economic losses (76.57 %) comes from the municipalities of Chía and Cajicá. Overall, losses for this scenario represent 21 % of the region GDP.

- The mean expected economic losses of the 18 scenarios range between USD 322.99 and 1517.56 million, which represent 5.17 % and 24.29 % of the replacement cost of the building inventory, which represent between 8 % and 38 % of the region's GDP.
- Incorporating the SV plays an important role in loss estimation. The adjusted economic losses for the 18 scenario regions range between USD 437 and 2093 million, on average a 36.6 % increase compared to the losses from building damage.

Overall, these results show that a seismic event corresponding to the design earthquake (475-year return period) would cause significant damage to the infrastructure and severe economic and social losses. Given the prevalence of unreinforced masonry houses, an effective mitigation strategy for this region is to develop seismic retrofitting programs for these buildings, especially for municipalities with higher population growth, which contribute the most to damage and losses.

Table 14. Expected economic losses in the region for each of the 18 scenarios considered. Economic losses when including SV consider the percentage of losses with respect to the total losses per municipality and are adjusted with the SVI.

Scenario	Direct economic losses		Economic losses with SV	
	Losses (USD in millions)	Percentage of losses (%)	Losses after considering the SVI (USD in millions)	Losses + SVI (%)
5.35 Tenjo	322.99	5.17	437.28	7.00
5.55 Cota	434.35	6.95	588.35	9.42
5.65 Zipaquirá	426.26	6.82	592.19	9.48
5.95 Chía	900.49	14.41	1240.72	19.86
5.95 Gachancipá	438.62	7.02	599.55	9.60
5.95 Tenjo	461.39	7.38	615.75	9.85
6.15 Tocancipá	571.58	9.15	778.38	12.46
6.25 Nemocón	484.05	7.75	660.98	10.58
6.25 Sopó	1181.64	18.91	1628.70	26.07
6.25 Tabio	824.01	13.19	1120.51	17.93
6.35 Cajicá	1295.51	20.73	1790.78	28.66
6.35 Cogua	794.91	12.72	1101.68	17.63
6.45 Cogua	1154.40	18.47	1596.73	25.55
6.55 Sopó	1450.55	23.21	2002.18	32.04
6.65 Nemocón	888.24	14.22	1211.52	19.39
6.65 Tabio	1343.27	21.50	1824.25	29.19
6.85 Tocancipá	695.64	11.13	949.69	15.20
6.95 Cota	1517.56	24.29	2093.23	33.50

The development of this study revealed two prominent areas for future research. The first is developing a robust framework to incorporate SV into the loss estimations, with a strong basis on how each social category should be weighted. Second, despite a careful selection of the fragility functions based on a literature review, the estimations of this study can be further refined by using a more complete dataset with fragility functions developed explicitly for Colombia, particularly for older masonry houses.

Code and data availability. The building surveys have been made available in the open repository available at https://dataservices.gfz-potsdam.de/panmetaworks/review/53f33a3960011189ac4d99e5719752e0ab02e9723f4743597e544faea0ecc720/ (Arroyo et al., 2022).

Author contributions. DF carried out most of the analyses, developed the risk scenarios and wrote the main body of the manuscript; JC assisted in the development of the exposure models, drawing figures, and the writing and formatting of the article. OA contributed to the conceptualization of the whole paper and proofreading the manuscript; DC contributed in the methodology and analysis of social vulnerability; TC helped with the development of the risk scenarios in OpenQuake. JV helped in the development of the hazard model, its analysis and figures of the article. All authors reviewed the manuscript and contributed to the interpretation of the results.

Competing interests. The contact author has declared that none of the authors has any competing interests.

Disclaimer. Publisher's note: Copernicus Publications remains neutral with regard to jurisdictional claims in published maps and institutional affiliations.

Special issue statement. This article is part of the special issue "Multi-risk assessment in the Andes region". It is not associated with a conference.

Acknowledgements. We would like to thank the Colombian Geological Survey for their support in the characterization of the hazard for the study area. We thank the Universidad de la Sabana, especially the work team of Sabana Centro Cómo Vamos for the data made available for the social vulnerability assessment. Our gratitude also goes to Fabrice Cotton for the advice during the elaboration of this study. We also thank Kevin Fleming for the careful proofreading of a previous draft.

Financial support. This research has been supported by the Universidad de La Sabana (grant no. ING-293-2021), the Engineering and Physical Sciences Research Council (grant no. EP/P025641/1), and the Bundesministerium für Bildung und Forschung (grant no. 03G0905A-H). Tamara Cabrera was funded by the Research

Center for Integrated Disaster Risk Management (CIGIDEN, grant no. ANID/FONDAP/15110017).

Review statement. This paper was edited by Jörn Lauterjung and reviewed by Pablo Heresi, Maria Camila Hoyos Ramirez, and Ana Acevedo.

References

Abrahamson, N. A., Silva, W. J., and Kamai, R.: Summary of the ASK14 Ground Motion Relation for Active Crustal Regions, Earthq. Spectra, 30, 1025–1055, https://doi.org/10.1193/070913eqs198m, 2014.

Acevedo, A. B., Jaramillo, J. D., Yepes, C., Silva, V., Osorio, F. A., and Villar, M.: the seismic risk of the unreinforced masonry building stock in Antioquia, Colombia, Nat. Hazards, 86, 31–54, https://doi.org/10.1007/S11069-016-2647-8, 2017.

Acevedo, A. B., Yepes-Estrada, C., González, D., Silva, V., Mora, M., Arcila, M., and Posada, G.: Seismic risk assessment for the residential buildings of the major three cities in Colombia: Bogotá, Medellín, and Cali, Earthq. Spectra, 36, 298–320, https://doi.org/10.1177/8755293020942537, 2020.

Arcila, M. M., García, J., Montenjo, J. S., Eraso, J. F., Valcárcel, J. A., Mora, M. G., Viganò, D., Pagani, M., and Díaz, F. J.: Modelo nacional de amenaza sísmica para Colombia, libros del Servicio Geológico Colombiano, https://doi.org/10.32685/9789585279469, 2020.

Arroyo, O., Barros, J., and Ramos, L.: Comparison of the Reinforced-Concrete Seismic Provisions of the Design Codes of the United States, Colombia, and Ecuador for Low-Rise Frames, Earthq. Spectra, 34, 441–458, https://doi.org/10.1193/102116eqs178ep, 2019.

Arroyo, O., Feliciano, D., Gomez Zapata, J. C., Shinde, S., and Brinckmann, N.: RRVS Building survey for building exposure modelling in Chía (Colombia) V. 1.0, GFZ Data Services [data set], https://dataservices.gfz-potsdam.de/panmetaworks/review/53f33a3960011189ac4d99e5719752e0ab02e9723f4743597e544faea0ecc720/ (last access: 15 January 2023), 2022.

Asociación Colombiana de Ingeniería Sísmica (AIS): Estudio General de Amenaza Sísmica de Colombia, Comité AIS-300: Amenaza sísmica, ISBN 978-958-97609-6-3, 2009.

Asociación Colombiana de Ingeniería Sísmica (AIS): Normas Colombianas de Diseño y Construcción Sismo-Resistente, NSR-10, ISBN 978-958-97609-3-2, 2010.

Bazzurro, P. and Cornell, C. A.: Disaggregation of seismic hazard, B. Seismol. Soc. Am., 89, 501–520, https://doi.org/10.1785/BSSA0890020501, 1999.

Bernal Granados, G. A.: Metodología para la modelación, cálculo y calibración de parámetros de la amenaza sísmica para la evaluación probabilista del riesgo, Universitat Politécnica de Catalunya, TDX (Tesis Doctorals en Xarxa), http://hdl.handle.net/10803/284898 (last access: 28 November 2022), 2014.

Bonet, J., Gerson, M., Pérez-Valbuena, J., and Chiriví-Bonilla, E. J.: Informalidad laboral y en la vivienda: primeros indicios para las principales ciudades colombianas, Documentos de Trabajo Sobre Economía Regional y Urbana, https://doi.org/10.32468/dtseru.241, 2016.

Bonett Díaz, R. L.: Vulnerabilidad y riesgo siìsmico de edificios aplicacioìn a entornos urbanos en zonas de amenaza alta y moderada. Universitat Politécnica de Catalunya, TDX (Tesis Doctorals en Xarxa), http://www.tdx.cat/handle/10803/6230 (last access: 9 October 2022), 2003.

Boot, E., Saito, K., and Madabhushi, G.: The Haiti earthquake of 12 January 2010, A field report by EEFIT, Vol. 12, https://www.istructe.org/IStructE/media/Public/Resources/report-eefit-portauprince-haiti-20190816.pdf (last access: 16 May 2023), 2010.

Brzev, S., Scawthorn, C., Charleson, A., Allen, L., Greene, M., Jaiswal, K., and Silva, V.: GEM global earthquake model GEM Building Taxonomy Version 2.0 exposure modelling, GEM Technical Report, https://doi.org/10.13117/GEM.EXP-MOD.TR2013.02, 2013.

Build Change, Colombia: https://buildchange.org/locations/colombia/, last access: 6 November 2021.

Burton, C. G. and Silva, V.: Assessing Integrated Earthquake Risk in OpenQuake with an Application to Mainland Portugal, Earthq. Spectra, 32, 1383–1403, 2016.

Calvi, G. M., Pinho, R., Magenes, G., Bommer, J. J., Restrepo-Vélez, L. F., and Crowley, H.: Development of seismic vulnerability assessment methodologies over the past 30 years, ISET Journal of Earthquake Technology, 43, 75–104, 2006.

Cardona, O., Wilches, G., García, X., Mansilla, E., Ramírez, F., and Marulanda, M.: Estudio sobre desastres ocurridos en Colombia: Estimación de pérdidas y cuantificación de costos, Evaluación de Riesgos Naturales – Colombia (ERN), 2004.

Carreño, M. L., Cardona, O. D., and Barbat, A. H.: Urban Seismic Risk Evaluation: A Holistic Approach, Nat. Hazards, 40, 137–172, https://doi.org/10.1007/S11069-006-0008-8, 2007.

Carreño, M. L., Cardona, O. D., Barbat, A. H., Suarez, D. C., Perez, M. P., and Narvaez, L.: Holistic Disaster Risk Evaluation for the Urban Risk Management Plan of Manizales, Colombia, Int. J. Disast. Risk Sc., 8, 258–269, https://doi.org/10.1007/S13753-017-0136-7, 2017.

Cauzzi, C., Faccioli, E., Vanini, M., and Bianchini, A.: Updated predictive equations for broadband (0.01–10 s) horizontal response spectra and peak ground motions, based on a global dataset of digital acceleration records, B. Earthq. Eng., 13, 1587–1612, https://doi.org/10.1007/s10518-014-9685-y, 2014.

Chaulagain, H., Silva, V., Rodrigues, H., Spacone, E., and Varum, H.: Earthquake loss estimation for the Kathmandu valley, Second European Conference on Earthquake Engineering and Seismology (2ECEES), 25–29 August 2014, Istanbul, Turkey, ISBN 978-1-5108-1021-1, 2014.

Chaulagain, H., Rodrigues, H., Silva, V., Spacone, E., and Varum, H.: Seismic risk assessment and hazard mapping in Nepal, Nat. Hazards, 78, 583–602, https://doi.org/10.1007/S11069-015-1734-6, 2015.

Chávez-García, F. J., Monsalve-Jaramillo, H., and Vila-Ortega, J.: Vulnerability and site effects in earthquake disasters in Armenia (Colombia) – Part 2 : Observed damage and vulnerability, Nat. Hazards Earth Syst. Sci., 21, 2345–2354, https://doi.org/10.5194/nhess-21-2345-2021, 2021.

Chen, W., Cutter, S. L., Emrich, C. T., and Shi, P.: Measuring social vulnerability to natural hazards in the Yangtze River

Delta region, China, Int. J. Disast. Risk Sc., 4, 169–181, https://doi.org/10.1007/s13753-013-0018-6, 2013.

Choi, Y. and Stewart, J. P.: Nonlinear site amplification as function of 30 m shear wave velocity, Earthq. Spectra, 21, 1–30, https://doi.org/10.1193/1.1856535, 2005.

Contreras, D.: Fuzzy Boundaries Between Post-Disaster Phases: The Case of L'Aquila, Italy, Int. J. Disast. Risk Sc., 7, 277–292, https://doi.org/10.1007/s13753-016-0095-4, 2016.

Contreras, D.: Popayan, the white city in Colombia, 35 years after the earthquake, https://dcontrerasster.wixsite.com/website/single-post/2016/05/03/Architecture-where-design-meets-engineering (last access: 23 January 2022), 2018.

Contreras, D., Wilkinson, S., Balan, N., Phengsuwan, J., and James, P.: Assessing Post-Disaster Recovery Using Sentiment Analysis. The case of L'Aquila, Haiti, Chile and Canterbury, 7th world conference on earthquake engineering (17WCEE), 13–18 September 2020, Sendai, Japan, 2020a.

Contreras, D., Chamorro, A., and Wilkinson, S.: Review article: The spatial dimension in the assessment of urban socioeconomic vulnerability related to geohazards, Nat. Hazards Earth Syst. Sci., 20, 1663–1687, https://doi.org/10.5194/nhess-20-1663-2020, 2020b.

Contreras, D., Voets, A., Junghardt, J., Bhamidipati, S., and Contreras, S.: The Drivers of Child Mortality During the 2012–2016 Drought in La Guajira, Colombia, In. J. Disast. Risk Sc., 11, 87–104, https://doi.org/10.1007/S13753-020-00255-0, 2020c.

Cotton, F., Scherbaum, F., Bommer, J. J., and Bungum, H.: Criteria for Selecting and Adjusting Ground-Motion Models for Specific Target Regions: Application to Central Europe and Rock Sites, J. Seismol., 10, 137–156, https://doi.org/10.1007/s10950-005-9006-7, 2006.

Cutter, S. L. and Finch, C.: Temporal and spatial changes in social vulnerability to natural hazards, P. Natl. Acad. Sci. USA, 105, 2301–2306, https://doi.org/10.1073/PNAS.0710375105, 2008.

Cutter, S. L., Boruff, B. J., and Shirley, W. L.: Social vulnerability to environmental hazards, Soc. Sci. Quart., 84, 242–261, https://doi.org/10.1111/1540-6237.8402002, 2003.

DANE: Censo Nacional de Población y Vivienda 2018, https://www.dane.gov.co/index.php/estadisticas-por-tema/demografia-y-poblacion/censo-nacional-de-poblacion-y-vivenda-2018 (last access: 18 January 2022), 2018.

Derras, B., Bard, P. Y., and Cotton, F.: VS30, slope, H800 and f0: Performance of various site-condition proxies in reducing ground-motion aleatory variability and predicting nonlinear site response, Earth Planets Space, 69, 1–21, https://doi.org/10.1186/S40623-017-0718-Z, 2017.

Eraso, J. and Montejo, J.: Mapa de V30 Integrado para Colombia. Escala 1: 3 000 000, Versión año 2019, Report from Servicio Geológico Colombiano (SGC), https://miig.sgc.gov.co/Paginas/Resultados.aspx?k=Vs30 (last access: 25 February 2022), 2020.

Erdik, M., Aydinoglu, N., Fahjan, Y., Sesetyan, K., Demircioglu, M., Siyahi, B., Durukal, E., Ozbey, C., Biro, Y., Akman, H., and Yuzugullu, O.: Earthquake risk assessment for Istanbul metropolitan area, Earthq. Eng. Eng. Vib., 2, 1–23, https://doi.org/10.1007/bf02857534, 2003.

Fatemi, F., Ardalan, A., Aguirre, B., Mansouri, N., and Mohammadfam, I. Social vulnerability indicators in disasters: Findings from a systematic review, Int. J. Disast. Risk Re., 22, 219–227, https://doi.org/10.1016/j.ijdrr.2016.09.006, 2017.

Feliciano, D., Arroyo, O., Liel, A., Carrillo, J., and Murray, P.: A framework to assess the seismic vulnerability of informally constructed houses: a case study in Villavicencio, Colombia, Proceedings of the 12th National Conference in EarthquakeEngineering, Earthquake Engineering Research Institute, 12th National Conference on Earthquake Engineering, 27 June–1 July, Salt Lake City, USA, 2022.

Freudenberg, M.: Composite Indicators of Country Performance: A Critical Assessment, Organisation for Economic Co-operation and Development (OECD), Paris, France, https://doi.org/10.1787/405566708255, 2003.

Field, A.: Discovering statistics using SPSS, Sage publications, Chenai, ISBN 9781526445780, 2005.

Gallego Silva, M.: Estimación del Riesgo Sísmico en la República de Colombia, https://repositorio.unam.mx/contenidos/ (last access: 3 January 2022), Repositorio Institucional de la UNAM, 2000.

Gentile, R. and Galasso, C.: Accounting for directivity-induced pulse-like ground motions in building portfolio loss assessment, B. Earthq. Eng., 19, 6303–6328, https://doi.org/10.1007/s10518-020-00950-9, 2021.

Gomez-Zapata, J. C., Brinckmann, N., Harig, S., Zafrir, R., Pittore, M., Cotton, F., and Babeyko, A.: Variable-resolution building exposure modelling for earthquake and tsunami scenario-based risk assessment: an application case in Lima, Peru, Nat. Hazards Earth Syst. Sci., 21, 3599–3628, https://doi.org/10.5194/nhess-21-3599-2021, 2021.

Haas, M., Wieland, M., and Pittore, M.: DEMO: Remote Rapid Visual Screening (RRVS), https://vimeo.com/158600573 (last access: 14 February 2023), GFZ – Early Warning Systems, 2016.

Heresi, P. and Miranda, E.: Evaluation of relative seismic performance between one-and two-story houses, J. Earthq. Eng., 26, 857–886, https://doi.org/10.1080/13632469.2019.1693447, 2022a.

Heresi, P. and Miranda, E.: Structure-to-structure damage correlation for scenario-based regional seismic risk assessment, Struct. Saf., 95, 102155, https://doi.org/10.1016/j.strusafe.2021.102155, 2022b.

Hoyos, M. C. and Hernández, A. F.: Impact of vulnerability assumptions and input parameters in urban seismic risk assessment, B. Earthq. Eng., 19, 4407–4434, https://doi.org/10.1007/S10518-021-01140-X, 2021.

Idriss, I. M.: An NGA-West2 empirical model for estimating the horizontal spectral values generated by shallow crustal earthquakes, Earthq. Spectra, 30, 1155–1177, https://doi.org/10.1193/070613eqs195m, 2014.

JICA: The study on disaster prevention in the Bogota metropolitan area in the Republic of Colombia, https://libopac.jica.go.jp/images/report/P0000055260.html (last access: 10 November 2021), 2002.

Joumard, I. and Londoño Vélez, J.: Income Inequality and Poverty in Colombia – Part 1. The Role of the Labour Market, OECD Economics Department Working Papers, No. 1036, https://doi.org/10.1787/5k487n74s1f1-en, 2013.

Lomnitz, C. and Hashizume, M.: The Popayán, Colombia, earthquake of 31 March 1983, B. Seismol. Soc. Am., 75, 1315–1326, https://doi.org/10.1785/bssa0750051315, 1985.

Macdonald, J., Junillon, C., Parker, G., and Taucer, F.: The Quindiìo, Colombia earthquake of 25 January 1999: a field report by EEFIT, Earthquake Engineering Field Investigation Team, 95 pp., ISBN 1874266565, 2000.

Martins, L. and Silva, V.: Development of a fragility and vulnerability model for global seismic risk analyses, B. Earthq. Eng., 19, 6719–6745, https://doi.org/10.1007/s10518-020-00885-1, 2021.

Michel, C., Hannewald, P., Lestuzzi, P., Fäh, D., and Husen, S.: Probabilistic mechanics-based loss scenarios for school buildings in Basel (Switzerland), B. Earthq. Eng., 15, 1471–1496, https://doi.org/10.1007/s10518-016-0025-2, 2017.

Murray, P. B., Feliciano, D., Goldwyn, B. H., Liel, A. B., Arroyo, O., and Javernick-Will, A.: Seismic safety of informally constructed reinforced concrete houses in Puerto Rico, Earthquake, 39, 5–33, https://doi.org/10.1177/87552930221123085, 2022.

Naciones Unidas – CEPAL: El terremoto de enero de 1999 en Colombia: impacto socioeconómico del desastre en la zona del eje cafetero, https://repositorio.cepal.org/handle/11362/25388 (last access: 12 December 2021), 1999.

Nievas, C. I., Pilz, M., Prehn, K., Schorlemmer, D., Weatherill, G., and Cotton, F.: Calculating earthquake damage building by building: the case of the city of Cologne, Germany, B. Earthq. Eng., 20, 1519–1565, https://doi.org/10.1007/s10518-021-01303-w, 2022.

OpenQuake Platform – Vulnerability: List of fragility functions, https://platform.openquake.org/vulnerability/list, last access: 27 November 2021.

Páez, H. M., López, S. A., P., N. A., Cadena, J. R., Hurtado, E. S., and Trenkamp, R.: Análisis geodésico y deformación sismotectónica asociada al sismo de Quetame, Colombia, 24 de mayo de 2008, Boletín Geológico, 43, 7–22, https://doi.org/10.32685/0120-1425/boletingeo.43.2015.26, 2015.

Pagani, M., Monelli, D., Weatherill, G. A. and Garcia, J.: The OpenQuake-engine Book: Hazard, Global Earthquake Model (GEM) Technical Report 2014-08, GEM Foundation, https://doi.org/10.13117/-GEM.OPENQUAKE.TR2014.08 , 2014.

PAHO: Disasters Preparedness and Mitigation in the Americas – Issue No. 17, News and information for the International Disaster Community, ISSN 0251-4494, 1983.

Paris, G., Machette, M. N., Dart, R. L., and Haller, K. M.: Map and Database of Quaternary Faults and Folds in Colombia and its Offshore Regions, Open-File Report 00-0284, A project of the International Lithosphere Program Task Group II-2, Major Active Faults of the World, USGS science for a changing world, 2000.

Pittore, M., Haas, M., and Megalooikonomou, K. G.: Risk-Oriented, Bottom-Up Modeling of Building Portfolios with Faceted Taxonomies, Frontiers in Built Environment, 4, 41, https://doi.org/10.3389/fbuil.2018.00041, 2018.

Pittore, M., Haas, M., and Silva, V.: Variable resolution probabilistic modeling of residential exposure and vulnerability for risk applications, Earthq. Spectra, 36, 321–344, https://doi.org/10.1177/8755293020951582, 2020.

Prieto, G. A., Beroza, G. C., Barrett, S. A., López, G. A., and Flórez, M.: Earthquake nests as natural laboratories for the study of intermediate depth earthquake mechanics, Tectonophysics, 570–571, 42–56, https://doi.org/10.1016/j.tecto.2012.07.019, 2012.

Sabana Centro cómo Vamos: Informe de Calidad de Vida 2018, Equipo del Observatorio, http://sabanacentrocomovamos.org/home/4to-informe-de-calidad-de-vida-de-sabana-centro/ (last access: 8 January 2022), 2019.

Salcedo, E. and Gómez, A.: Estudio Macrosísmico del terremoto del 18 de octubre de 1743 en la región central de Colombia, Boletín de Geología, 35, 109–128, http://www.scielo.org.co/scielo.php?script=sci_arttext&pid=S0120-02832013000100009 (last access: 30 October 2022), 2013.

Salgado, M. A., Zuloaga, D., Bernal, G. A., Mora, M. G., and Cardona, O. D., Fully probabilistic seismic risk assessment considering local site effects for the portfolio of buildings in Medellín, Colombia, B. Earthq. Eng., 12, 671–695, https://doi.org/10.1007/S10518-013-9550-4, 2014.

Salgado, M. A., Bernal, G. A., Zuloaga, D., Marulanda, M. C., Cardona, O. D., and Henao, S.: Probabilistic Seismic Risk Assessment in Manizales, Colombia: Quantifying Losses for Insurance Purposes, Int. J. Disast. Risk Sc., 8, 296–307, https://doi.org/10.1007/S13753-017-0137-6, 2017.

Scherbaum, F., Bommer, J. J., Bungum, H., Cotton, F., and Abrahamson, N. A.: Composite ground-motion models and logic trees: methodology, sensitivities, and uncertainties, B. Seismol. Soc. Am., 95, 1575–1593, 2005.

Schmidtlein, M. C., Shafer, J. M., Berry, M., and Cutter, S. L.: Modeled earthquake losses and social vulnerability in Charleston, South Carolina, Appl. Geogr., 31, 269–281, https://doi.org/10.1016/j.apgeog.2010.06.001, 2011.

Servicio Geológico Colombiano (SGC): Sismicidad Histórica de Colombia, http://sish.sgc.gov.co/visor/sesionServlet?metodo=irAIntensidadesSismo&idSismo=25, last access: 26 November 2021a.

Servicio Geológico Colombiano (SGC): Catálogo Sísmico Integrado, http://bdrsnc.sgc.gov.co/paginas1/catalogo/index.php, last access: 27 November 2021b.

Silva, V.: Critical Issues in Earthquake Scenario Loss Modeling, J. Earthq. Eng., 20, 1322–1341, https://doi.org/10.1080/13632469.2016.1138172, 2016.

Silva, V., Crowley, H., Varum, H., and Pinho, R.: Seismic risk assessment for mainland Portugal, B. Earthq. Eng., 13, 429–457, https://doi.org/10.1007/s10518-014-9630-0, 2014a.

Silva, V., Crowley, H., Pagani, M., Monelli, D., and Pinho, R.: Development of the OpenQuake engine, the Global Earthquake Model's open-source software for seismic risk assessment, Nat. Hazards, 72, 1409–1427, https://doi.org/10.1007/s11069-013-0618-x, 2014b.

Stewart, J. P., Douglas, J., Javanbarg, M., Bozorgnia, Y., Abrahamson, N. A., Boore, D. M., Campbell, K. W., Delavaud, E., Erdik, M., and Stafford, P. J.: Selection of ground motion prediction equations for the global earthquake model, Earthq. Spectra, 31, 19–45, https://doi.org/10.1193/013013eqs017m, 2015.

Türker, E., Cotton, F., Pilz, M., and Weatherill, G.: Analysis of the 2019 M_w 5.8 Silivri Earthquake Ground Motions: Evidence of Systematic Azimuthal Variations Associated with Directivity Effects, Seismol. Res. Lett., 93, 693–705, https://doi.org/10.1785/0220210168, 2022.

Villar-Vega, M. and Silva, V.: Assessment of earthquake damage considering the characteristics of past events in South America, Soil Dyn. Earthq. Eng., 99, 86–96, https://doi.org/10.1016/j.soildyn.2017.05.004, 2017.

Villar-Vega, M., Silva, V., Crowley, H., Yepes, C., Tarque, N., Acevedo, A. B., Hube, M. A., Gustavo, C. D., and Santa María, H.: Development of a fragility model for the residential building stock in South America, Earthq. Spectra, 33, 581–604, https://doi.org/10.1193/010716eqs005m, 2017.

Weatherill, G. A., Silva, V., Crowley, H., and Bazzurro, P.: Exploring the impact of spatial correlations and uncertainties for portfolio analysis in probabilistic seismic loss estimation, B. Earthq. Eng., 13, 957–981, https://doi.org/10.1007/s10518-015-9730-5, 2015.

World Bank: Data, https://datos.bancomundial.org/, last access: 16 January 2022.

Yepes-Estrada, C., Silva, V., Valcárcel, J., Acevedo, A. B., Tarque, N., Hube, M. A., Coronel, G., and Santa María, H.: Modeling the Residential Building Inventory in South America for Seismic Risk Assessment, Earthq. Spectra, 33, 299–322, https://doi.org/10.1193/101915eqs155dp, 2017.